JOURNAL OF BACTERIOLOGY, Jan. 2010, p. 242–255 Vol. 192, No. 1
0021-9193/10/$12.00 doi:10.1128/JB.01244-09

Discovery and Characterization of Three New *Escherichia coli* Septal Ring Proteins That Contain a SPOR Domain: DamX, DedD, and RlpA▽

S. J. Ryan Arends,[1] Kyle Williams,[1] Renada J. Scott,[1]† Silvana Rolong,[1]‡ David L. Popham,[2] and David S. Weiss[1]*

Department of Microbiology, The University of Iowa, Iowa City, Iowa 52242,[1] and Department of Biological Sciences, Virginia Tech, Blacksburg, Virginia 24061[2]

Received 15 September 2009/Accepted 22 October 2009

SPOR domains are ~70 amino acids long and occur in >1,500 proteins identified by sequencing of bacterial genomes. The SPOR domains in the FtsN cell division proteins from *Escherichia coli* and *Caulobacter crescentus* have been shown to bind peptidoglycan. Besides FtsN, *E. coli* has three additional SPOR domain proteins—DamX, DedD, and RlpA. We show here that all three of these proteins localize to the septal ring in *E. coli*. The loss of DamX or DedD either alone or in combination with mutations in genes encoding other division proteins resulted in a variety of division phenotypes, demonstrating that DamX and DedD participate in cytokinesis. In contrast, RlpA mutants divided normally. Follow-up studies revealed that the SPOR domains themselves localize to the septal ring in vivo and bind peptidoglycan in vitro. Even SPOR domains from heterologous organisms, including *Aquifex aeolicus*, localized to septal rings when produced in *E. coli* and bound to purified *E. coli* peptidoglycan sacculi. We speculate that SPOR domains localize to the division site by binding preferentially to septal peptidoglycan. We further suggest that SPOR domain proteins are a common feature of the division apparatus in bacteria. DamX was characterized further and found to interact with multiple division proteins in a bacterial two-hybrid assay. One interaction partner is FtsQ, and several synthetic phenotypes suggest that DamX is a negative regulator of FtsQ function.

Cell division in *Escherichia coli* is mediated by a collection of approximately 20 proteins, all of which localize to the midcell, where they form a structure called the septal ring, or divisome. About half of these proteins are essential for cell division. The corresponding temperature-sensitive mutants or depletion strains become filamentous and die under nonpermissive conditions. The remaining proteins are not essential under most laboratory conditions. In some cases null mutations reveal modest division defects, but in other cases division defects become apparent only under certain growth conditions or in combination with mutations in genes for other division proteins. For reviews of this topic, see references 18, 22, 29, and 67.

One of the essential cell division proteins is a bitopic membrane protein named FtsN (see Fig. 1A) (13, 14). How FtsN facilitates cell division is not clear. Because overproduction of FtsN rescues a variety of mutants with lesions in genes for other cell division proteins [*ftsA*(Ts), *ftsI*(Ts) *ftsQ*(Ts), *ftsEX* null, *ftsK* null, and *ftsP* (*sufI*) null strains], it seems likely that one function of FtsN is to improve the assembly and/or stability of the septal ring (13, 20, 24, 30, 58, 63). Very recent evidence indicates that FtsN plays an important role in triggering constriction, probably by allosteric activation of some other component of the septal ring (26).

A notable feature of FtsN is that it contains at its C terminus a peptidoglycan (PG) binding domain known as a SPOR domain (Pfam accession no. 05036) (23, 65, 72). SPOR domains are both common and widespread in bacteria. At the time of this writing (August 2009), over 1,500 proteins that contain a SPOR domain are listed in the Pfam database (23). These proteins come from over 500 bacterial species. The domain is named after the founding member of the protein family, a *Bacillus subtilis* protein named CwlC that is produced relatively late in the process of sporulation (41). CwlC, which comprises an N-terminal amidase domain and a C-terminal SPOR domain, facilitates release of the mature spore by degrading PG in the mother cell (48, 61).

Our interest in SPOR domain proteins was piqued during a study of *Vibrio parahaemolyticus* (in collaboration with Linda McCarter) when we observed that a gene of unknown function, designated *vpa1294*, is highly induced in *V. parahaemolyticus* swarmer cells. The VPA1294 protein was annotated as a "putative DamX-related protein" (44; http://genome.gen-info.osaka-u.ac.jp/bacteria/vpara/). To learn about DamX, we turned to the EcoGene website (http://ecogene.org/) (57), which noted that (i) DamX from *E. coli* has an essentially unknown function, (ii) overproduction of DamX inhibits cell division (43), and (iii) DamX is one of four *E. coli* proteins that contain a SPOR domain, the others being the cell division protein FtsN and two proteins of unknown function, DedD and RlpA. Based on this information, we decided to investigate whether DamX, DedD, and RlpA are involved in cell division in *E. coli*. While this work was in progress, the Thanbichler laboratory demonstrated that *Caulobacter crescentus* has an FtsN-like protein that is needed for cell division (49) and the de Boer laboratory published a report on DamX, DedD, and RlpA from *E. coli* (26). We also learned that J. Maddock's

* Corresponding author. Mailing address: Department of Microbiology, Carver College of Medicine, The University of Iowa, Iowa City, IA 52242. Phone: (319) 335-7785. Fax: (319) 335-9006. E-mail: david-weiss@uiowa.edu.

† Present address: 2583 Bristol Cove, Horn Lake, MS 38637.

‡ Present address: 8911 SW 123 Ct. Apt. 210, Miami, FL 33186.

▽ Published ahead of print on 30 October 2009.

laboratory has been investigating DamX, DedD, and RlpA from *E. coli* (personal communication). Importantly, the major findings from all four laboratories are in general agreement: SPOR domain proteins are widespread in bacteria, many of these proteins are involved in cell division, and SPOR domains are sufficient for septal localization, probably because SPOR domains bind to septal PG.

MATERIALS AND METHODS

Media. *E. coli* strains were grown in Luria-Bertani (LB) medium containing 10 g tryptone, 5 g yeast extract, and 10 g NaCl per liter. For LB0N medium, NaCl was omitted. Plates contained 15 g agar per liter. Antibiotics were used at the following concentrations: 200 μg ampicillin/ml, 30 μg chloramphenicol/ml, 40 μg kanamycin/ml, and 100 or 35 μg spectinomycin/ml for plasmids or chromosomal alleles, respectively.

Strains. Strains used in this study are listed in Table 1. *Aquifex aeolicus* DNA was obtained from R. Huber, *Cytophaga hutchinsonii* ATCC 33406 was obtained from the American Type Culture Collection, and *V. parahaemolyticus* LM5674 was obtained from L. McCarter. Eviction of antibiotic cassettes by using pCP20, integration of CRIM (conditional-replication, integration, and modular) plasmids into the chromosome, and P1-mediated transduction were done according to procedures described previously (11, 15, 34, 47). All *kan* evictions left behind an *frt* scar.

(i) Strains for phenotypic analysis of *damX*, *dedD*, and *rlpA* mutants. The Keio collection strains JW3351 (*damX*<>*kan*), JW3578 (*dedD*<>*kan*), and JW0628 (*rlpA*<>*kan*) were obtained and verified by diagnostic PCR as described previously (2, 15). Strains EC1793, EC1794, and EC1795 were constructed using pCP20 to evict *kan* from JW3351, JW3578, and JW0628. EC1910, EC1912, and EC1914 were constructed using transduction to introduce *damX*<>*kan*, *dedD*<>*kan*, or *rlpA*<>*kan* from JW3351, JW3578, or JW0628 into EC251. Strains EC1916, EC1918, EC1920, EC1922, EC1924, and EC1926 were constructed using transduction to introduce *damX*<>*kan*, *dedD*<>*kan*, or *rlpA*<>*kan* from JW3351, JW3578, or JW0628 into EC1793, EC1794, or EC1795. Strains EC1928 and EC1929 were constructed by transforming EC1793 and EC1795 with pDSW998. EC1930 and EC1932 were constructed using pCP20 to evict *kan* from EC1916 and EC1920. Strains EC1934 and EC1936 were constructed using transduction to introduce *dedD*<>*kan* from JW3578 into EC1928 and EC1929. EC1938 and EC1939 were constructed using electroporation to introduce pDSW998 into EC1930 and EC1932. Strains EC1940 and EC1941 were constructed using pCP20 to evict *kan* from EC1934 and EC1936. Strains EC1942, EC1944, EC1946, and EC1948 were constructed by transduction to introduce *dedD*<>*kan*, *rlpA*<>*kan*, or *damX*<>*kan* from JW3351, JW3578, or JW0628 into EC1938, EC1939, EC1940, or EC1941. Strains EC2150, EC2152, EC2154, and EC2156 were constructed using pDSW390 to bump out pDSW998 from EC1942, EC1944, EC1946, and EC1948.

(ii) Strains for localization of green fluorescent protein (GFP)-DamX or GFP-DedD in wild-type or mutant backgrounds. The CRIM plasmids pDSW983 (P_{204}::*gfp-damX*) and pDSW984 (P_{204}::*gfp-dedD*) were integrated into the chromosomes of EC251, EC295, EC297, EC303, EC309, EC1908, EC1924, JW3351, and JW3578. The resulting strains were designated EC2138, EC2139, EC2140, EC2142, EC2144, EC2146, EC2148, EC2130, EC2132, and EC2177.

(iii) Strains to screen for synthetic phenotypes of *damX*<>*kan* with other *fts* mutations. P1 transduction was used to move *damX*<>*kan* from JW3351 into EC294, EC295, EC297, EC303, EC309, and PS223. The resulting strains were designated EC1986, EC1988, EC1990, EC1992, EC1994, and EC1996, respectively.

(iv) Other strains. EC295 and EC303 were constructed by transduction to introduce *ftsI23*(Ts) together with *leu*::Tn*10* and *ftsQ1*(Ts) together with *leu*::Tn*10*, respectively, into EC251. The donor strains were LMG64 and MJC129 (33).

Plasmids. Plasmids used in this study are listed in Table 2. In the following descriptions, primer-carried restriction sites are underlined.

(i) Plasmids that encode GFP or red fluorescent protein (RFP) fusions to full-length SPOR domain proteins. pDSW918 (P_{204}::*gfp-damX*) was constructed by amplifying *damX* from EC251 chromosomal DNA with primers P1136 (CAGCAATTGAACAACAACATGGATGAATTCAAACCAGAAGAC) and P1137 (CTGAAGCTTACTTCAGATCGGCCTGTACCT). The 1,312-bp product was cut with MfeI and HindIII and ligated into pDSW207 that had been digested with EcoRI and HindIII. The fusion joins GFP to DamX via a 5-amino-acid (5-aa) linker, ELNNN. pDSW929 (P_{206}::*vpa1294-mcherry*) was constructed by amplifying *vpa1294* from chromosomal DNA of *V. parahaemolyticus* strain LM5674 with primers VPA1294Up (CAGGAATTCGTGCACAAGATTTTAT CTTTGACAT) and VPA1294Down (GTCTCTAGAGTTGTTGTTGCGCATT CTCACGACACTAGTT). The 429-bp product was cut with EcoRI and XbaI and ligated into the corresponding sites of pDSW913. The fusion construct changes the N terminus of VPA1294 from MHK to MEFVHK, and there is a 5-aa linker, SRNNN, between VPA1294 and mCherry. pDSW931 (P_{206}::*rlpA-mcherry*) was constructed by amplifying *rlpA* from EC251 chromosomal DNA with primers P1140 (CAGGAATTCATGCGTAAGCAGTG GCTCGGGA) and P1141 (GTCTCTAGAGTTGTTGTTCTGCGCGGTAG TAATAAATGAC). The 1,113-bp product was cut with EcoRI and XbaI and ligated into pDSW913 that had been cut with the same enzymes. The fusion construct adds the tripeptide MEF to the N terminus of RlpA, and there is a 5-aa linker, SRNNN, between RlpA and mCherry. pDSW937 (P_{204}::*gfp-dedD*) was constructed by amplifying *dedD* from EC251 chromosomal DNA with primers P1138 (CAGGAATTCAACGTGGCAAGTAAGTTTCAGAATCG) and P1139 (GACA AGCTTAATTCGGCGTATAGCCCATTAC). The 682-bp product was cut with EcoRI and HindIII and ligated into pDSW207 that had been digested with the same enzymes. The fusion joins GFP to DedD via a one-Asn-residue linker and replaces the initiating Met of DedD with Val. pDSW983 allows for integration of P_{204}::*gfp-damX* into the chromosome at the ϕ80 *att* site. It was constructed by digesting pDSW918 with SphI and ScaI. The 4,322-bp fragment that carried *lacI*^{q} and P_{204}::*gfp-damX* was ligated into pJC69 that had been cut with SphI and HincII. pDSW984 (P_{204}::*gfp-dedD*) was constructed similarly using a 3,692-bp SphI-ScaI fragment from pDSW937.

(ii) Plasmids that encode fusions of the TorA signal sequence and GFP to isolated SPOR domains. pDSW992, expressing a fusion protein comprising Tat-targeted GFP (^{TT}GFP) and FtsN residues 240 to 319 under the control of P_{204} [P_{204}::^{TT}*gfp-ftsN*(240–319)], was constructed by amplifying the last 80 codons of *ftsN* with primers P1123 (GCCGGATCCAACAACAACGCGGA GAAAAAAGACGAA) and P761 (CCCAAGCTTTCAACCCCCGGCGGC GAGCCG) and plasmid pDSW433 as the template. The 270-bp product was cut with BamHI and HindIII and ligated into the corresponding sites of pDSW962. pDSW994 [P_{204}::^{TT}*gfp-dedD*(141–220)] was constructed by amplifying the last 80 codons of *dedD* from plasmid pDSW937 with primers P1125 (GCCGGATCCAACAACAACGGTAAAGCCTATGTTGTG) and P1126 (GCCAAGCTTTAATTCGGCGTATAGCCCATT). The 269-bp product was cut with BamHI and HindIII and ligated into the corresponding sites of pDSW962. pDSW995 [P_{204}::^{TT}*gfp-rlpA*(283–362)] was constructed by amplifying the last 80 codons of *rlpA* from plasmid pDSW931 with primers P1127 (GCCAGATCTAAC AACAACGTCTCGCAAAGCGCCAGC) and P1128 (GCCAAGCTTTACTGCG CGGTAGTAATAAAT). The 269-bp product was cut with BglII and HindIII and ligated into the BamHI and HindIII sites of pDSW962. An analogous fusion protein comprising GFP and the last 80 residues of DamX did not localize to the septal ring, so we constructed a longer fusion protein that included the last 91 residues of DamX, which localized well. The corresponding plasmid, pDSW997 [P_{204}::^{TT}*gfp-damX*(338–428)], was constructed using primers P1144 (GCCGGATCCAACAACAACGGTTCGTTGAAATCGGCA) and P1137 (CT GAAGCTTACTTCAGATCGGCCTGTACCT) with pDSW918 as the template. The 301-bp product was cut with BamHI and HindIII and ligated into the corresponding sites of pDSW962. pDSW1067 [P_{204}::^{TT}*gfp-aq1896*(254–342)] was constructed by amplifying the last 89 codons of *aq1896* from *A. aeolicus* chromosomal DNA with primers P1223 (GCCGGATCCAACAACAACATCCCAA GAGTGCATAAA) and P1224 (CTGAAGCTTATCACTTGATTTCAACGAC GAA). The 298-bp product was cut with BamHI and HindIII and ligated into the corresponding sites of pDSW962. pDSW1069 [P_{204}::^{TT}*gfp-chu2221*(161–249)] was constructed by amplifying the last 89 codons of *chu2221* from chromosomal DNA of *C. hutchinsonii* ATCC 33406 with primers P1229 (GCCGGATCCAA CAACAACTTCTATTCTACTAAATTGGAG) and P1230 (CTGAAGCTTAT TTTGGAGATAGGATCACACT). The 295-bp product was cut with BamHI and HindIII and ligated into the corresponding sites of pDSW962.

(iii) Plasmids for overproduction of His$_6$-tagged SPOR domains. Plasmids for the overproduction of His$_6$-tagged SPOR domains were constructed as described above for ^{TT}GFP-SPOR domain plasmids except that the region encoding the SPOR domain of VPA1294 was amplified using primers P1317 (GCCGGATC CAACAACAACGCATACGGCTACCTGAATCCC) and P1318 (CTGAAGC TTAGCGCATTCTCACGACACTAG). The PCR products were ligated into pQE80L. All constructs carry the vector-derived sequence MRGSHHHHHHG SNNN at the N terminus.

(iv) Other plasmids. pDSW433 (P_{BAD}::*ftsN*) was constructed by amplifying *ftsN* from a pBAD24-*ftsN* construct (lab collection) with primers P353 (GACT CTAGATCAACCCCCGGCGGC) and P354 (CTTGAGCTCGAGGAATTCA CCATGGCACAAC). The 990-bp product was cut with SacI and XbaI and

TABLE 1. Strains used in this study

Strain	Relevant features[a]	Source or reference
BL21(λ DE3)	*ompT gal dcm hsdS$_B$*(r_B^- m_B^-) λ (P_{lacUV5}::T7 gene 1)	Novagen
BW25113	*rrnB3* Δ*lacZ4787 hsdR514* Δ(*araBAD*)*567* Δ(*rhaBAD*)*568 rph-1*	2
DHM1	*glnV44*(AS) *recA1 endA gyrA96 thi-1 hsdR17 spoT1 rfbD1 cya-854*	38
EC251	K-12 wild type MG1655	Lab collection
EC295	EC251 *ftsI23*(Ts) *leu*::Tn*10*	This study
EC297	EC251 *ftsA12*(Ts) *leu*::Tn*10*	21
EC303	EC251 *ftsQ1*(Ts) *leu*::Tn*10*	This study
EC309	EC251 *ftsZ84*(Ts) *leu*::Tn*10*	63
EC1793	BW25113 Δ*damX*	This study
EC1794	BW25113 Δ*dedD*	This study
EC1795	BW25113 Δ*rlpA*	This study
EC1908	EC251 P_{BAD}::*ftsN* (Km^r)	63
EC1910	EC251 *damX*<>*kan*	This study
EC1912	EC251 *dedD*<>*kan*	This study
EC1914	EC251 *rlpA*<>*kan*	This study
EC1916	BW25113 Δ*damX rlpA*<>*kan*	This study
EC1918	BW25113 Δ*dedD rlpA*<>*kan*	This study
EC1920	BW25113 Δ*rlpA damX*<>*kan*	This study
EC1922	BW25113 Δ*rlpA dedD*<>*kan*	This study
EC1924	BW25113 Δ*damX dedD*<>*kan*	This study
EC1926	BW25113 Δ*dedD damX*<>*kan*	This study
EC1928	BW25113 Δ*damX*/pDSW998 (P_{BAD}::*dedD* Cm^r)	This study
EC1929	BW25113 Δ*rlpA*/pDSW998 (P_{BAD}::*dedD* Cm^r)	This study
EC1930	BW25113 Δ*damX* Δ*rlpA*	This study
EC1932	BW25113 Δ*damX* Δ*rlpA*	This study
EC1934	BW25113 Δ*damX dedD*<>*kan*/pDSW998 (P_{BAD}::*dedD* Cm^r)	This study
EC1936	BW25113 Δ*rlpA dedD*<>*kan*/pDSW998 (P_{BAD}::*dedD* Cm^r)	This study
EC1938	BW25113 Δ*damX* Δ*rlpA*/pDSW998 (P_{BAD}::*dedD* Cm^r)	This study
EC1939	BW25113 Δ*damX* Δ*rlpA*/pDSW998 (P_{BAD}::*dedD* Cm^r)	This study
EC1940	BW25113 Δ*damX* Δ*dedD*/pDSW998 (P_{BAD}::*dedD* Cm^r)	This study
EC1941	BW25113 Δ*rlpA* Δ*dedD*/pDSW998 (P_{BAD}::*dedD* Cm^r)	This study
EC1942	BW25113 Δ*damX* Δ*rlpA dedD*<>*kan*/pDSW998 (P_{BAD}::*dedD* Cm^r)	This study
EC1944	BW25113 Δ*damX* Δ*rlpA dedD*<>*kan*/pDSW998 (P_{BAD}::*dedD* Cm^r)	This study
EC1946	BW25113 Δ*damX* Δ*dedD rlpA*<>*kan*/pDSW998 (P_{BAD}::*dedD* Cm^r)	This study
EC1948	BW25113 Δ*rlpA* Δ*dedD damX*<>*kan*/pDSW998 (P_{BAD}::*dedD* Cm^r)	This study
EC1986	EC251 *leu*::Tn*10 damX*<>*kan*	This study
EC1988	EC251 *ftsI23*(Ts) *leu*::Tn*10 damX*<>*kan*	This study
EC1990	EC251 *ftsA12*(Ts) *leu*::Tn*10 damX*<>*kan*	This study
EC1992	EC251 *ftsQ1*(Ts) *leu*::Tn*10 damX*<>*kan*	This study
EC1994	EC251 *ftsZ84*(Ts) *leu*::Tn*10 damX*<>*kan*	This study
EC1996	W3110 *zipA1*(Ts) *damX*<>*kan*	This study
EC2130	BW25113 *damX*<>*kan* ϕ80::pDSW983 (P_{204}::*gfp-damX* Sp^r)	This study
EC2132	BW25113 *dedD*<>*kan* ϕ80::pDSW984 (P_{204}::*gfp-dedD* Sp^r)	This study
EC2138	EC251 ϕ80::pDSW983 (P_{204}::*gfp-damX* Sp^r)	This study
EC2139	EC251 ϕ80::pDSW984 (P_{204}::*gfp-dedD* Sp^r)	This study
EC2140	EC251 *ftsZ84*(Ts) *leu*::Tn*10* ϕ80::pDSW983 (P_{204}::*gfp-damX* Sp^r)	This study
EC2142	EC251 *ftsA12*(Ts) *leu*::Tn*10* ϕ80::pDSW983 (P_{204}::*gfp-damX* Sp^r)	This study
EC2144	EC251 *ftsQ1*(Ts) *leu*::Tn*10* ϕ80::pDSW983 (P_{204}::*gfp-damX* Sp^r)	This study
EC2146	EC251 *ftsI23*(Ts) *leu*::Tn*10* ϕ80::pDSW983 (P_{204}::*gfp-damX* Sp^r)	This study
EC2148	EC251 P_{BAD}::*ftsN kan* ϕ80::pDSW983 (P_{204}::*gfp-damX* Sp^r)	This study
EC2150	BW25113 Δ*damX* Δ*rlpA dedD*<>*kan*/pDSW390	This study
EC2152	BW25113 Δ*damX* Δ*rlpA dedD*<>*kan*/pDSW390	This study
EC2154	BW25113 Δ*damX* Δ*dedD rlpA*<>*kan*/pDSW390	This study
EC2156	BW25113 Δ*rlpA* Δ*dedD damX*<>*kan*/pDSW390	This study
EC2177	BW25113 Δ*damX dedD*<>*kan* ϕ80::pDSW983(P_{204}::*gfp-damX* Sp^r)	This study
JW3351	BW25113 *damX*<>*kan*	2
JW3578	BW25113 *dedD*<>*kan*	2
JW0628	BW25113 *rlpA*<>*kan*	2
PS223	W3110 *zipA1*(Ts)	54

[a] AS, amber suppressor.

ligated into the corresponding sites of pBAD33. The resulting construct endowed *ftsN* with a Shine-Dalgarno sequence and a start codon derived in part from pBAD24. pDSW913 (P_{206}::multiple-cloning site [MCS]-*mcherry*) is a vector for fusing the mCherry variant of RFP to the C termini of target proteins. It was constructed by amplifying *mcherry* from plasmid pMalp2-mCherry (a gift from Greg Phillips, Iowa State University) with primers P991 (GTCAAAGCTTTTACTTGTACAGCTCGTCCATG) and P992 (GTCATCTAGAATGGTGAGCAAGGGCGAGGA). The 731-bp fragment was digested with HindIII and XbaI and ligated into the corresponding sites of pDSW206. To construct pDSW966 (P_{lac}::T25-*damX*) and pDSW968 (P_{lac}::T18-*damX*), *damX* was amplified by PCR

TABLE 2. Plasmids used in this study

Plasmid	Relevant features[a]	Source or reference
pBAD33	Arabinose regulation (P_{BAD}); p15A ori Cm^r	32
pDSW204	IPTG regulation (P_{204}); *lacI*^{q} pBR ori Ap^r	68
pDSW206	IPTG regulation (P_{206}); *lacI*^{q} pBR ori Ap^r	68
pDSW207	*gfp* fusion vector (pDSW204-*gfp*-MCS)	68
pDSW390	*gfp* fusion vector (P_{206}::*gfp*-MCS *lacI*^{q} p15A ori Ap^r)	Lab collection
pDSW433	pBAD33-*ftsN*	Lab collection
pDSW913	*rfp* fusion vector (pDSW206-MCS-*mcherry*)	This study
pDSW918	P_{204}::*gfp-damX lacI*^{q} *bla* pBR ori	This study
pDSW929	P_{206}::*vpa1294-rfp lacI*^{q} *bla* pBR ori	This study
pDSW931	P_{206}::*rlpA-rfp lacI*^{q} *bla* pBR ori	This study
pDSW937	P_{204}::*gfp-dedD lacI*^{q} *bla* pBR ori	This study
pDSW962	^{TT}*gfp* fusion vector (P_{204}::^{ss}*torA-gfp lacI*^{q} *bla* pBR ori)	63
pDSW966	P_{lac}::*cya*$^{1–675}$-*damX kan* p15A ori (pKT25-*damX*)	This study
pDSW967	P_{lac}::*cya*$^{1–675}$-*dedD kan* p15A ori (pKT25-*dedD*)	This study
pDSW968	P_{lac}::*cya*$^{675–1197}$-*damX bla* pBR ori (pUT18c-*damX*)	This study
pDSW969	P_{lac}::*cya*$^{675–1197}$-*dedD bla* pBR ori (pUT18c-*dedD*)	This study
pDSW983	P_{204}::*gfp-damX lacI*^{q} Sp^r (pJC69 derivative)	This study
pDSW984	P_{204}::*gfp-dedD lacI*^{q} Sp^r (pJC69 derivative)	This study
pDSW992	P_{204}::^{TT}*gfp-ftsN*(240–319) *lacI*^{q} *bla*	This study
pDSW994	P_{204}::^{TT}*gfp-dedD*(141–220) *lacI*^{q} *bla*	This study
pDSW995	P_{204}::^{TT}*gfp-rlpA*(283–362) *lacI*^{q} *bla*	This study
pDSW997	P_{204}::^{TT}*gfp-damX*(338–428) *lacI*^{q} *bla*	This study
pDSW998	pBAD33-*dedD*	This study
pDSW1000	pQE80L-*damX*(338–428)	This study
pDSW1002	pQE80L-*dedD*(141–220)	This study
pDSW1003	pQE80L-*rlpA*(283–362)	This study
pDSW1113	pQE80L-*chu2221*(161–249)	This study
pDSW1114	pQE80L-*aq1869*(254–342)	This study
pDSW1115	pQE80L-*vpa1294*(37–134)	This study
pDSW1067	P_{204}::^{TT}*gfp-aq1896*(254–342) *lacI*^{q} *bla*	This study
pDSW1069	P_{204}::^{TT}*gfp-chu2221*(161–249) *lacI*^{q} *bla*	This study
pJC69	oriR6Kγ *attP* ϕ80 Sp^r (CRIM vector)	8
pET-3Z$^+$	$P_{T7gene10}$::*ftsZ* Ap^r pBR ori	55
pKT25	BACTH vector for fusion of target proteins to *Bordetella pertussis cya* gene T25 fragment; P_{lac}::*cya*$^{1–675}$ p15 ori Km^r	40
pKT25-*ftsA*	P_{lac}::*cya*$^{1–675}$-*ftsA*	38
pKT25-*ftsB*	P_{lac}::*cya*$^{1–675}$-*ftsB*	38
pKT25-*ftsI*	P_{lac}::*cya*$^{1–675}$-*ftsI*	38
pKT25-*ftsL*	P_{lac}::*cya*$^{1–675}$-*ftsL*	38
pKT25-*ftsN*	P_{lac}::*cya*$^{1–675}$-*ftsN*	38
pKT25-*ftsQ*	P_{lac}::*cya*$^{1–675}$-*ftsQ*	38
pKT25-*ftsW*	P_{lac}::*cya*$^{1–675}$-*ftsW*	38
pKT25-*ftsX*	P_{lac}::*cya*$^{1–675}$-*ftsX*	38
pKT25-*ftsZ*	P_{lac}::*cya*$^{1–675}$-*ftsZ*	38
pKT25-*zip*	P_{lac}::*cya*$^{1–675}$-*zip* (construct encoding leucine zipper from GCN4)	39
pQE80L	Carries T5 promoter and *lac* operators; *lacI*^{q} ColE1 ori Ap^r	Qiagen
pUT18c	BACTH vector for fusion of target proteins to *B. pertussis cya* gene T18 fragment; P_{lac}::*cya*$^{675–1197}$-MCS pUC ori Ap^r	40
pUT18c-*ftsA*	P_{lac}::*cya*$^{675–1197}$-*ftsA*	38
pUT18c-*ftsB*	P_{lac}::*cya*$^{675–1197}$-*ftsB*	38
pUT18c-*ftsI*	P_{lac}::*cya*$^{675–1197}$-*ftsI*	38
pUT18c-*ftsL*	P_{lac}::*cya*$^{675–1197}$-*ftsL*	38
pUT18c-*ftsN*	P_{lac}::*cya*$^{675–1197}$-*ftsN*	38
pUT18c-*ftsQ*	P_{lac}::*cya*$^{675–1197}$-*ftsQ*	38
pUT18c-*ftsW*	P_{lac}::*cya*$^{675–1197}$-*ftsW*	38
pUT18c-*ftsX*	P_{lac}::*cya*$^{675–1197}$-*ftsX*	38
pUT18c-*zip*	P_{lac}::*cya*$^{675–1197}$-*zip* (construct encoding leucine zipper from GCN4)	39

[a] Residues encoded by *cya* gene fragments are indicated by superscript numbers. ^{ss}*torA*, TorA signal sequence construct; BACTH, bacterial two-hybrid system.

from EC251 chromosomal DNA with primers P1076 (CTAGAGGATCCCATGGATGAATTCAAACCAG) and P1077 (CTTAGGTACCTTACTTCAGATCGGCCTG). The 1,286-bp fragment was cut with BamHI and KpnI and ligated into pKT25 and pUT18c that had been cut with the same enzymes. Likewise, to construct pDSW967 (P_{lac}::T25-*dedD*) and pDSW969 (P_{lac}::T18-*dedD*), *dedD* was amplified by PCR using primers P1078 (CTAGAGGATCCCGTGGCAAGTAAGTTTCAG) and P1079 (CTTAGGTACCTTAATTCGGCGTATAGCC). The 663-bp PCR product was cut with BamHI and KpnI and ligated into the corresponding sites of pKT25 and pUT18c. pDSW998 is a pBAD33 derivative that expresses *dedD*. It was constructed using primers P1153 (GTGTCTAGAGTCGCACATGTCATGGAAGTG) and P1154 (GTGAAGCTTAATTCGGCGTATAGCCCATTACC) to am-

plify *dedD* from BW25113 chromosomal DNA. The resulting 719-bp product was cut with XbaI and HindIII and ligated into the corresponding sites of pBAD33.

Division phenotypes of *damX*, *dedD*, and *rlpA* mutants. Cultures grown overnight in LB medium were diluted 1:500 in the same medium and grown for 4 h at 30°C to an optical density at 600 nm (OD_{600}) of ~0.5, at which point the cells were fixed. To better observe chaining and invaginations, cells were stained with the membrane dye FM4-64. To assay for deoxycholate sensitivity, overnight cultures grown in LB medium were adjusted to an OD_{600} of 1.0 in LB0N medium and then fourfold serial dilutions were made and 3-μl aliquots were spotted onto an LB0N agar plate containing 0.01 mM IPTG (isopropyl-β-D-thiogalactopyranoside) and 0.1% deoxycholate. Plates were photographed after 18 h at 30°C.

Rescue of *ftsQ1*(Ts) mutant by *damX<>kan*. Plating efficiency was assessed by spotting dilutions of cultures onto LB0N medium. One milliliter of overnight culture grown in LB medium was centrifuged, and the resulting cell pellet was taken up into 1 ml of LB0N medium. This culture was then diluted to a starting OD_{600} of 1.0, and a series of 10-fold serial dilutions in LB0N medium was prepared. Four microliters of each dilution was spotted onto plates containing LB0N medium, and the plates were incubated at 42°C for 16 h before being photographed. Division efficiency was assessed by phase-contrast microscopy. Overnight cultures were diluted 1:50 into LB medium and grown for 2 h at 30°C. These cultures, now in exponential growth, were then diluted 1:6 into LB0N medium, grown for 1 h at 42°C, fixed, and photographed.

Protein localization. Live cells were used in all cases for studies of protein localization. (i) Strains expressing full-length SPOR proteins fused to GFP carried IPTG-inducible fusions stably integrated into the chromosome, so antibiotic selection was not necessary. Cultures grown overnight in LB medium were diluted 1:500 into LB medium containing 0.1 mM IPTG and grown for 4 h at 30°C to an OD_{600} of ~0.5, at which point they were spotted onto thin agarose pads (63). (ii) Strains expressing full-length SPOR proteins fused to RFP were cultured similarly except that ampicillin was included to maintain plasmids and 1 mM IPTG was used to induce production of the fusion protein. (iii) Strains expressing fusions of GFP to isolated SPOR domains were grown similarly except that ampicillin was included to maintain plasmids, IPTG was omitted because basal expression proved sufficient, and overnight cultures were diluted 1:50 and grown for 2 h before microscopy.

Localization dependency studies. Live cells were used in all cases for localization dependency studies. To localize GFP-DamX in temperature-sensitive strains, overnight cultures were diluted 1:50 into LB medium and grown for 2 h at 30°C. These cultures were then diluted 1:6 under permissive conditions (LB medium at 30°C) or nonpermissive conditions (LB0N medium at 42°C) and grown for 60 to 90 min. To visualize GFP-DamX in cells depleted of FtsN, cultures were grown overnight in LB medium containing 0.2% L-arabinose. The next morning, cultures were diluted 1:50 into LB medium containing 0.2% D-glucose and grown for 2 h at 30°C to an OD_{600} of ~0.5. These cultures were then diluted 1:50 into permissive medium (LB medium with arabinose and 0.1 M IPTG) or nonpermissive medium (LB medium with glucose and 0.1 M IPTG) and grown for 3 to 4 h, by which time the glucose-grown cells were filamentous. To localize GFP-DamX in a *damX dedD<>kan* double mutant, overnight cultures were diluted 1:500 into LB medium containing various concentrations of IPTG and grown to an OD_{600} of ~0.5.

General microscopy methods. Our microscope, camera, and software have been described previously, as has the immobilization of live cells on agarose pads (1, 46, 63). The mCherry variant of RFP was visualized using the filter set we used previously for Texas Red and FM4-64 (70).

Bacterial two-hybrid assay. Transformants of DHM1 carrying appropriate plasmid pairs (derivatives of pUT18c and pKT25) were streaked onto plates of LB medium containing ampicillin (200 μg/ml) and kanamycin (40 μg/ml), and the plates were incubated for 2 or 3 days at 30°C. Three to five colonies were used to inoculate 5 ml of LB medium containing ampicillin and kanamycin plus 0.5 mM IPTG and grown on a roller at 30°C for ~16 h to an OD_{600} of 0.6 to 0.8. Then duplicate 15-μl culture samples were assayed for β-galactosidase activity by standard procedures (47). All assays were repeated at least three times (on different days).

Western blotting. For Western blotting, typically 1 ml of culture at an OD_{600} of ~0.5 was centrifuged and the resulting cell pellet was taken up into ~0.5 ml of sodium dodecyl sulfate-polyacrylamide gel electrophoresis (SDS-PAGE) loading buffer to achieve a sample concentration of 4.0 OD_{600} units per ml. Samples were boiled, and 10-μl aliquots were subjected to SDS–10% PAGE. Proteins were then transferred onto nitrocellulose and detected by standard methods. Rabbit anti-GFP antibodies were obtained from W. Margolin and C. Ellermeier and used at dilutions of 1:2,500 and 1:10,000, respectively. Rabbit anti-RFP serum (a gift from L. Shapiro) was used at a 1:10,000 dilution, and affinity-purified rabbit anti-FtsQ (10) was used at a 1:4,000 dilution. The secondary antibody was horseradish peroxidase-conjugated goat anti-rabbit antibody (1:8,000; Pierce, Rockford, IL), which in turn was detected with SuperSignal Pico West chemiluminescent substrate (Pierce, Rockford, IL). Blots were visualized with an LAS-1000 luminescent imager from Fuji (Stamford, CT).

Purified proteins. MBP2* was purchased from New England Biolabs (Beverly, MA). FtsZ was overproduced and purified as described previously (55), except that Q-Sepharose Fast-Flow was substituted for DEAE-Sephacel. His_6-tagged SPOR domains were overproduced in and purified from *E. coli* BL21(DE3) transformants by nickel affinity chromatography on Talon affinity resin according to instructions from the manufacturer (Clontech, Mountain View, CA). The purified proteins were dialyzed into storage buffer (50 mM Tris-HCl, 200 mM NaCl, 5% glycerol, pH 7.5), and aliquots were stored at −80°C until needed. A 0.5-liter culture yielded ~4 mg purified protein as determined by a bicinchoninic acid assay (Pierce) with bovine serum albumin as the standard. The purity was >95% as judged by SDS-PAGE.

Purification and quantification of PG. Whole PG sacculi were isolated from 1-liter cultures of EC251 after being boiled in SDS essentially as described previously (28). To quantify muramic acid, samples of purified PG were suspended in 6 N HCl and hydrolyzed at 95°C for 4 h. Hydrolysates were subjected to amino sugar analysis (31) and quantified relative to purified standards processed in parallel.

PG binding assays. Binding assays (65) were conducted with a solution of 25 mM potassium phosphate, pH 7.5, and 200 mM NaCl. A standard assay mixture contained 12 μg protein and 75 μg PG in a total volume of 100 μl. As a control, assay mixtures that lacked PG were also prepared. Mixtures were incubated for 1 h on ice and then centrifuged at 4°C in a Beckman TLA-55 rotor at 50,000 rpm (average *g* force, 112,000 × *g*) for 45 min. The PG pellet was washed by suspending it in 100 μl of cold assay buffer and centrifuging as described above. The PG pellet was again suspended in 100 μl of binding buffer. The supernatant from the initial binding step, the wash fluid, and the resuspended pellet were analyzed by SDS–15% PAGE. Gels were stained with GelCode blue (Pierce, Rockford, IL) and scanned using a Typhoon 8610 imager with the following instrument settings: excitation laser, 532 nm; emission filter, 560 nm, long pass; photomultiplier, 600 V; and pixel size, 100 μm. ImageQuant software was used to quantify fluorescence signals.

RESULTS

Overview of the *E. coli* SPOR domain proteins DamX, DedD, and RlpA. The *E. coli* SPOR domain proteins are diagrammed in Fig. 1A. DamX, DedD, and FtsN have similar overall structures. Each is a bitopic inner membrane protein with an N-terminal cytoplasmic domain, a single transmembrane helix, and a relatively large periplasmic domain, the last ~70 aa of which comprises a SPOR domain. RlpA, in contrast, is predicted to be an outer membrane lipoprotein. Alignments of the four proteins indicate that their homology is confined to the SPOR domains, which are only 18% identical in pairwise comparisons. Figure 1B compares the four *E. coli* SPOR domains and three heterologous SPOR domains included in this study.

Except for FtsN, the *E. coli* SPOR domain proteins have unknown functions. None of the proteins appear to be essential, as null mutants exist in the Keio collection and the corresponding genes did not turn up in a previous screen for essential genes in *E. coli* (2, 25). *damX* is named for its location next to the *dam* gene, which encodes DNA adenine methyltransferase (37). Overexpression of *damX* has been reported to interfere with cell division and alter biofilm formation (43, 64). DedD is named for *d*ownstream *E*. coli *D*NA, reflecting the discovery of this protein by sequencing downstream of *folC* (52). To our knowledge, no phenotypes have been associated with *dedD* mutants. RlpA is named for *r*are *l*ipo*p*rotein *A* (62), and *rlpA* is located in an operon with genes encoding PBP2 and RodA; the downstream gene encodes PBP5. All of these pro-

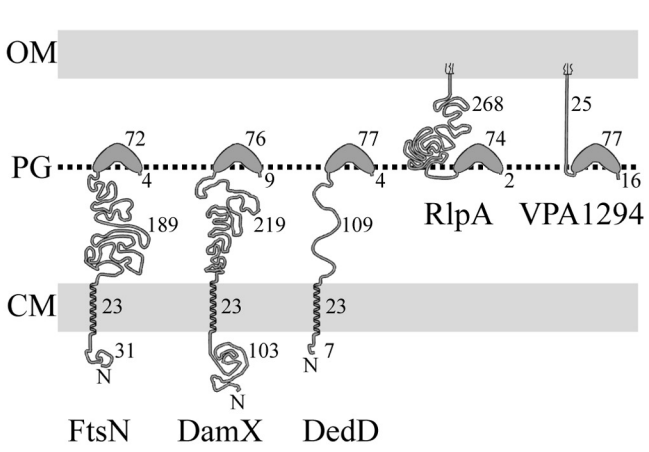

B

```
      FtsN 244 DERRWMVQCGSFRGAEQAETVRAQLAFEGFDS-----KITTNNGWNRVVIGPVKGKENADSTLNRLKMA--GHTNCIRL
      DamX 344 PSSHYTLQLSSSSNYDNLNGWAKKENLKNYVVYE---TTRNGQPWYVLVSGVYASKEEAKKAVSTLPADVQAKNPWAKP
      DedD 140 TGKAYVVQLGALKNADKVNEIVGKLRGAGYRVYTSP-STPVQGKITRILVGPDASKDKLKGSLGELKQL-SGLSGVVMG
      RlpA 287 ASGNFMVQVGAVSDQARAQQYQQQLGQKFGVPG----RVTQNGAVWRIQLGPFASKAEASTLQQRLQTE-AQLQSFITT
    VPA1294  42 NPNHYTMQVLALKKEKDVKEYIRYIDPKHPVWVNW--KNSRGTRWYTVTAGDFKSKQEAYNALSSLPSHVKQSSPFVLT
    CHU2221 171 RPKGYLLQIGAFSSYEHASRRIGELDDYTIGAPCIELITVKKKKLYRVIYSGFATKQKVTQKQKELKKK--GFDSVILS
     AQ1896 268 KEKYYAVQLGAFSTKERADKLVQELKSKGLRDL----RILPTDGVYKVIYGRFETPEEARRAKEEVKKL--GIYGFVVE
Consensus       ASGGYYVQLGAFSNEANAEALAAKLRAKGFAAKEA--VTSGGGGLYRVRVGPFASREEARAALKKLKAA--GLSPFVVR
```

FIG. 1. SPOR domain proteins included in this study. (A) Membrane topology and number of amino acids in each domain as retrieved from UniProt release 15.7 (http://www.uniprot.org) or the GTOP update of 15 December 2008 (http://spock.genes.nig.ac.jp/~genome/gtop.html). N, amino terminus; CM, cytoplasmic membrane; OM, outer membrane. RlpA and VPA1294 have a covalently attached lipid at their amino termini. (B) Multiple-sequence alignment of SPOR domains shown in the present study to localize to the septal ring of *E. coli*. Sequences were aligned manually to the position-specific scoring matrix (PSSM) from http://www.ncbi.nlm.nih.gov/Class/Structure/pssm/pssm_viewer.cgi with the SPOR domain (Pfam accession no. 05036) as the PSSM identifier (PSSM ID). Residues with identity to those in the consensus sequence from the PSSM alignment are shaded gray. Numbers to the left refer to the first positions of the SPOR domains in the indicated proteins.

teins are involved in cell wall metabolism and/or cell shape, suggesting that RlpA may be involved in these processes as well (3). Nevertheless, the only previously published data regarding a phenotype associated with RlpA is the finding that a truncated *rlpA* gene is a multicopy suppressor of a *prc* mutation (3). Prc, also known as Tsp, is a periplasmic protease that processes a variety of substrates that have nonpolar C termini, including the cell division protein FtsI (51).

DamX, DedD, and RlpA localize to the septal ring. To determine whether the uncharacterized *E. coli* SPOR domain proteins localize to the septal ring, we constructed IPTG-inducible fusions to the mut2 variant of GFP (12, 68) or the mCherry variant of RFP (9, 42, 59). We also constructed an RFP fusion to VPA1294, the *V. parahaemolyticus* protein that launched this investigation. The *gfp-damX* and *gfp-dedD* fusions were integrated into the chromosome in single copies, but our camera had difficulty detecting RFP when produced from the chromosome, so *rlpA-rfp* and *vpa1294-rfp* were expressed from plasmids.

Cells in exponential growth were immobilized on an agarose pad and visualized by fluorescence microscopy. Each of the SPOR domain proteins appeared as a bright band of fluorescence at the midcell, but in deeply constricting cells, the fluorescent signal was more reminiscent of a bright dot at the point of constriction (Fig. 2A and B). In the case of DamX, ~80% of the cells exhibited septal localization, suggesting that DamX is an early recruit to the septal ring. But only ~40% of cells exhibited septal DedD or R1pA, implying that these proteins are late recruits. In summary, we infer that the SPOR domain proteins localize to the septal ring prior to or at the onset of constriction and remain associated with the ring until division is complete.

Samples of the cultures examined by microscopy were also analyzed by Western blotting with anti-GFP and anti-RFP antibodies to verify that the fusion proteins were largely intact. As expected, the full-length fusion protein was the predominant species in all cases, although VPA1294-RFP was somewhat prone to proteolysis (Fig. 2C). For reasons that are not known, GFP-DamX consistently migrated more slowly than expected based on its predicted mass. We also verified that the GFP-DamX and GFP-DedD fusion proteins function in cell division (see below), but the functionality of RlpA-RFP could not be tested because we were unable to find any phenotypes associated with the loss of RlpA.

SPOR domains themselves localize to septal rings. The observation that DamX, DedD, RlpA, and VPA1294 localize to septal rings suggested that SPOR domains themselves localize to septal rings. This inference was particularly strong in the case of VPA1294, since it consists of a SPOR domain and little else (Fig. 1A). Moreover, FtsN′s SPOR domain was said to localize to division sites (P. de Boer, personal communication). We therefore constructed fusions of GFP to the SPOR domains of DamX, DedD, FtsN, and RlpA. These fusions were targeted to the periplasm by using a Tat signal sequence from TorA (4). As expected, septal localization was readily apparent in every case, and there was a tendency for production of

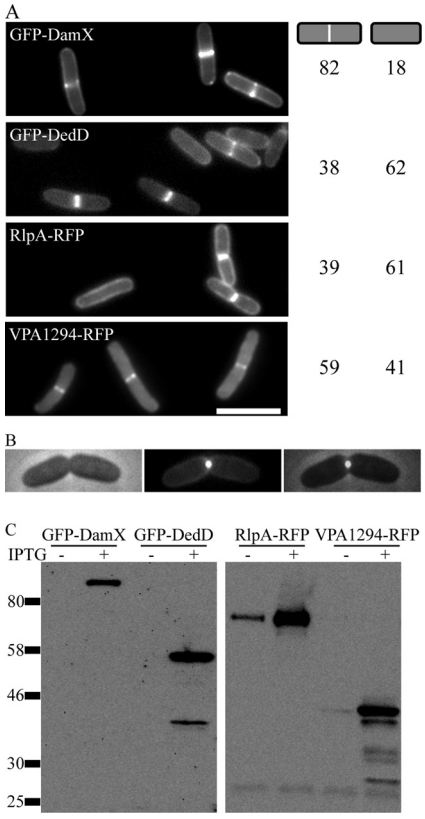

FIG. 2. Full-length SPOR domain proteins localize to the septal ring. (A) Fluorescence micrographs of live cells producing the indicated GFP or RFP fusion protein (left) and frequencies of septal localization (in percentages for ≥200 cells analyzed) in these cells (right). Bar, 5 μm. Cells were grown to an OD_{600} of ~0.5 in LB medium with 0.1 or 1 mM IPTG for GFP or RFP fusions, respectively. (B) Localization of GFP-DamX in a deeply constricted cell. Phase-contrast (left), fluorescence (middle), and overlay (right) micrographs. (C) Analysis of GFP and RFP fusion proteins by Western blotting. Whole-cell extracts were subjected to SDS-PAGE, transferred onto nitrocellulose, and probed with anti-GFP or anti-RFP. Predicted masses are as follows: GFP-DamX, 73.4 kDa; GFP-DedD, 50.1 kDa; RlpA-RFP, 65.2 kDa; and VPA1294-RFP, 40.6 kDa. For RlpA-RFP and VPA1294-RFP, these masses apply to the constructs after processing of the type II signal sequences. Molecular mass markers in kilodaltons are indicated to the left. The strains used were EC2130 (*damX*<>*kan* P_{204}::*gfp-damX*), EC2132 (*dedD*<>*kan* P_{204}::*gfp-dedD*), JW0628/pDSW931 (*rlpA*<>*kan* P_{206}::*rlpA-rfp*), and EC251/pDSW929 (wild type carrying P_{206}::*vpa1294-rfp* plasmid).

GFP-SPOR domain constructs to interfere with cell division (Fig. 3A). Septal localization depended on the presence of a SPOR domain because ^{TT}GFP (Tat-targeted GFP without a SPOR domain) exhibited only uniform periplasmic localization and did not impair division (data not shown, but see references 4 and 63). It should be noted that for the SPOR domains of DamX, DedD, and RlpA, localization was observed in null mutants, so the possibility that full-length DamX, DedD, or RlpA is needed to recruit the cognate SPOR domain to the septal ring can be excluded.

To determine how general this phenomenon might be, we investigated the localization of SPOR domains from two very distant relatives of *E. coli*. The organisms chosen were *C. hutchinsonii*, a soil bacterium belonging to the *Flavobacteria-*

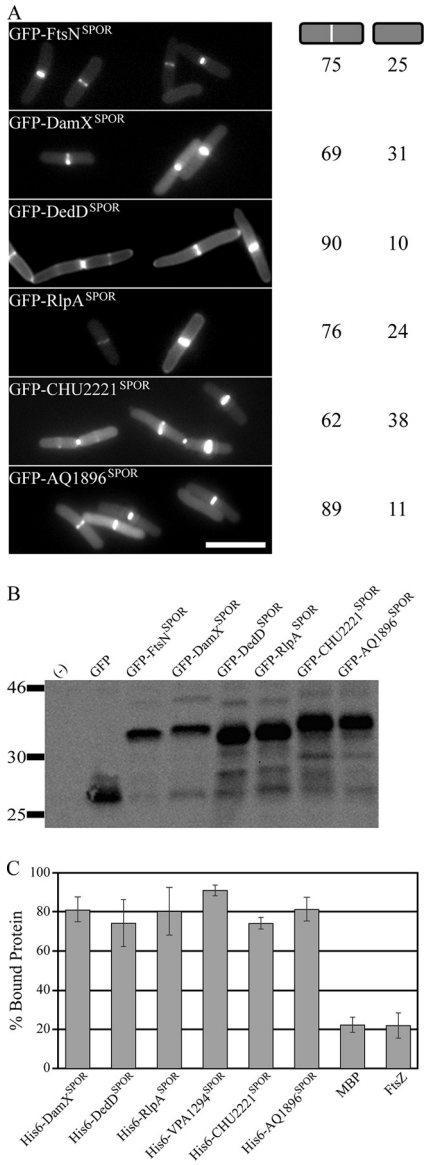

FIG. 3. SPOR domains localize to the septal ring and bind PG sacculi. (A) Fluorescence micrographs of live cells producing the indicated GFP fusion protein from a plasmid (left) and frequencies of septal localization (in percentages for ≥200 cells analyzed) in these cells (right). Cells were grown to an OD_{600} of ~0.5 in LB medium without IPTG. Bar, 5 μm. The strains shown are EC251/pDSW992 (expressing the fusion comprising GFP and the SPOR domain of FtsN [GFP-FtsN^{SPOR}]); JW3351/pDSW997 (expressing GFP-DamX^{SPOR}); JW3578/pDSW994 (expressing GFP-DedD^{SPOR}); JW0628/pDSW995 (expressing GFP-RlpA^{SPOR}); EC251/pDSW1069 (expressing GFP-CHU2221^{SPOR}); and EC251/pDSW1067 (expressing GFP-AQ1896^{SPOR}). (B) Analysis of GFP fusion proteins by Western blotting. Whole-cell extracts were subjected to SDS-PAGE, transferred onto nitrocellulose, and probed with anti-GFP. Molecular mass markers in kilodaltons are indicated to the left. The predicted masses of the various GFP-SPOR domain fusion proteins after export range from 36 to 38 kDa. The strains analyzed are as listed in the legend to panel A except that (−) indicates EC251 and GFP corresponds to EC251/pDSW962. (C) PG binding assay. Purified proteins were mixed with purified *E. coli* sacculi and subjected to ultracentrifugation to pellet the sacculi, which were washed and centrifuged again. Samples of the supernatant, the wash fluid, and the final pellet were analyzed by SDS-PAGE and Coomassie staining to determine what fraction of the input protein was in the final pellet. Bars indicate the averages and standard deviations of results from three independent experiments. MBP, maltose binding protein.

Bacteroides group (roughly as distant from *E. coli* as gram-positive organisms like *B. subtilis*), and *A. aeolicus*, which grows in hot springs (optimal temperature, 80°C) and is a member of the deepest branch in the domain *Bacteria* (16, 71), although there is evidence for extensive lateral gene transfer (5). Remarkably, both foreign SPOR domains localized efficiently and impaired cell division somewhat when produced in *E. coli* (Fig. 3A). Production of each SPOR domain construct was verified by Western blotting (Fig. 3B).

Many SPOR domains bind PG. We favor the notion that SPOR domains localize to division sites because they bind preferentially to septal PG (see Discussion). Nevertheless, to our knowledge, only the SPOR domains from FtsN proteins of *E. coli* and *C. crescentus* have actually been shown to bind PG (49, 65). In both cases, binding was demonstrated by showing that the purified SPOR domain copelleted with isolated PG sacculi upon ultracentrifugation. The SPOR domain from CwlC of *B. subtilis* has been reported previously to bind PG on the basis of nuclear magnetic resonance chemical shifts in certain protein residues elicited by the addition of PG fragments obtained by digesting sacculi with an amidase (48), but our analysis of the SPOR domain of DamX suggests that those chemical shifts were misinterpreted (K. Williams, A. Fowler, and D. Weiss, unpublished data).

To determine whether PG binding is a general property of SPOR domains, we purified His_6-tagged SPOR domains from DamX, DedD, RlpA, and the VPA1294, CHU2221, and AQ1896 proteins. The purified proteins were mixed with isolated PG sacculi and subjected to ultracentrifugation. Approximately 80% of the SPOR domain protein was recovered in the PG pellet (Fig. 3C), whereas all of the protein remained in the soluble fraction when the sample was centrifuged in the absence of PG (data not shown). As a negative control, we performed similar pulldown assays with maltose binding protein and FtsZ. In both cases, only ~20% of the protein copelleted with PG (Fig. 3C), and neither protein was detected in the pellet when the sample was centrifuged in the absence of PG (data not shown). We conclude that the SPOR domains under study are indeed PG binding proteins, as their affinities for PG in the pulldown assay are much higher than expected for proteins that bind PG only nonspecifically.

Placement of DamX in the recruitment hierarchy. Studies of Fts protein localization in cells with various *fts* mutant backgrounds have revealed a remarkably linear set of dependencies in *E. coli* (29, 66, 67). Although the physiological and mechanistic significance of these observations remains unclear, it is possible that the dependencies reflect, at least in part, a pathway for assembly of proteins into the septal ring. The dependencies also suggest which proteins are likely to interact with each other.

We introduced our IPTG-inducible *gfp-damX* fusion into the chromosomes of a set of strains in which division proteins other than DamX could be inactivated or depleted. Cells were grown under both permissive and nonpermissive conditions and immobilized on agarose pads, and fluorescence microscopy was used to assess the localization of GFP-DamX. The results are presented in Fig. 4 and Table 3. Inactivation of FtsZ prevented recruitment of GFP-DamX to potential division sites (Fig. 4A; Table 3). Western blotting revealed that the *ftsZ84*(Ts) mutant had appropriate amounts of GFP-DamX (Fig. 4B), so the lack of fluorescent bands can be attributed to a localization defect rather than a problem with the stability of the fusion protein. GFP-DamX localization was readily apparent in cells of all other mutant backgrounds tested (Fig. 4A; Table 3), including *ftsA12*(Ts) cells, although the fluorescent bands were sometimes ill defined, as if GFP-DamX was efficiently recruited to potential division sites but the septal rings were not well organized. These results imply that DamX fits into the dependency hierarchy at the same stage as FtsZ binding proteins such as FtsA, ZipA, and ZapA. Although we did not explicitly test the dependency of downstream division proteins on DamX, the fact that *damX* mutants are normal in length makes it very unlikely that DamX plays an important role in recruiting any of the essential downstream division proteins to the septal ring.

Two other noteworthy observations emerged from this set of experiments. First, GFP-DamX caused a mild chaining phenotype in cells with the *ftsQ1*(Ts) background, as if DamX is an inhibitor of FtsQ (Fig. 4A). Second, *gfp-damX* eliminated the division defect of a Δ*damX dedD<>kan* mutant, indicating that the *gfp-damX* fusion is functional (Fig. 4C). However, rescue from the defect was observed only at low levels of *gfp-damX* expression. If IPTG was increased to 0.1 mM to drive higher-level expression, *gfp-damX* caused striking filamentation in the Δ*damX dedD<>kan* mutant. Note that induction of *gfp-damX* with 0.1 mM IPTG was well tolerated in cells with other genetic backgrounds (Fig. 2A and 4A).

Cell division phenotypes of *damX*, *dedD*, and *rlpA* mutants suggest functional redundancy. We obtained and characterized *damX*, *dedD*, and *rlpA* null mutants from the Keio collection (2). In LB medium, the *dedD<>kan* mutant was somewhat elongated and had a slight chaining phenotype (Fig. 5A; Table 4). The *gfp-dedD* fusion used to demonstrate septal localization abolished both phenotypes (compare the mutant in Fig. 5A to the complemented mutant illustrating GFP-DedD localization in Fig. 2A). The division defects were milder in LB0N medium (data not shown). The *dedD<>kan* mutant was not sensitive to deoxycholate when plated on LB0N medium (Fig. 5B). This result implies that the outer membrane is intact. Deoxycholate sensitivity in PG hydrolase mutants with defects in septal PG synthesis and cell separation has been reported previously (35). The *damX<>kan* mutant did not have a visible division phenotype when grown on LB or LB0N medium (Fig. 5A; also data not shown) but was mildly sensitive to deoxycholate on LB0N medium, and the *gfp-damX* fusion abolished that phenotype (Fig. 5B). The *gfp-damX* fusion also eliminated the striking division defects (see below) observed in a *damX dedD* double mutant, provided the fusion was not too highly expressed (Fig. 4C). We were unable to find any division-related phenotype for the *rlpA<>kan* mutant, which did not elongate, chain, or exhibit sensitivity to deoxycholate (Fig. 5). Owing to the lack of a phenotype due to *rlpA<>kan*, we could not test whether the RlpA-RFP fusion protein was functional.

These mild phenotypes are not due to the Keio strains' having acquired suppressor mutations, because we observed similar phenotypes after using P1 transduction to move the alleles into cells with the MG1655 strain background from our laboratory collection (Table 4). Moreover, the phenotypes ob-

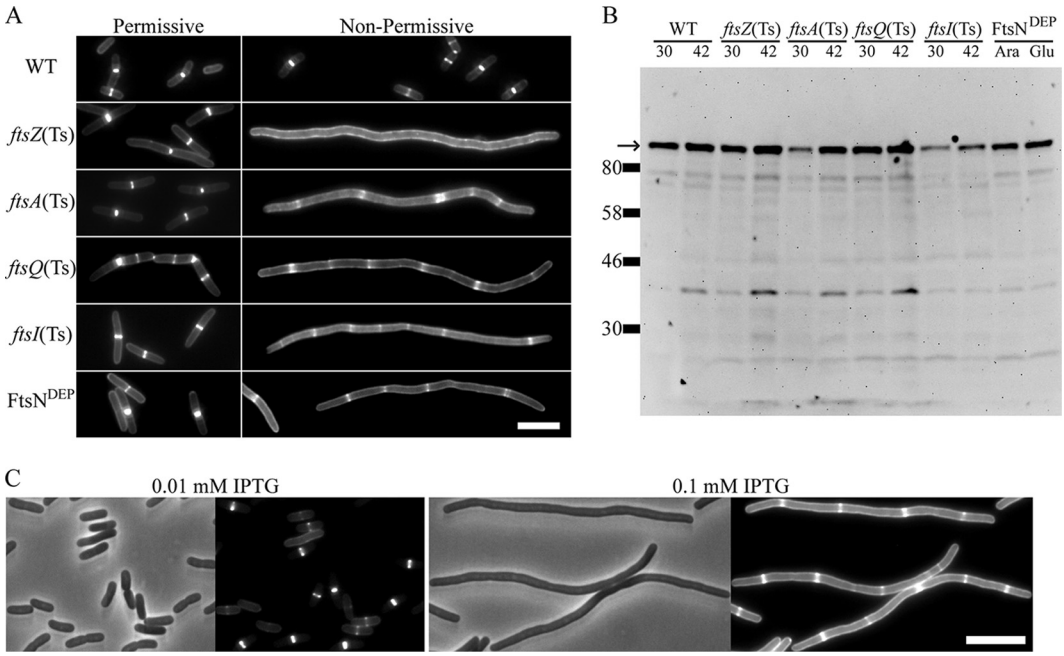

FIG. 4. Dependency of GFP-DamX localization on other septal ring proteins. (A) Fluorescence micrographs of live cells with the indicated genotypes or phenotypes grown under permissive conditions (30°C for temperature-sensitive mutants, with arabinose for the FtsN depletion [FtsN^{DEP}] strain) or nonpermissive conditions (42°C for temperature-sensitive mutants, with glucose for the FtsN depletion strain). IPTG was used at 0.1 mM in all cases to induce expression of *gfp-damX*. Bar, 5 μm; WT, wild type. (B) Western blot showing steady-state levels of GFP-DamX in cells pictured in panel A. Molecular mass markers in kilodaltons are indicated to the left of the blot. The black arrow points to the band corresponding to the GFP-DamX fusion. Strains used for analyses presented in panels A and B were as follows: WT, EC2138; *ftsZ*(Ts), EC2140; *ftsA*(Ts), EC2142; *ftsQ*(Ts), EC2144; *ftsI*(Ts), EC2146; and FtsN^{DEP}, EC2148. (C) Localization of GFP-DamX in a *damX dedD* double mutant. Phase-contrast and fluorescence micrographs of strain EC2177 (Δ*damX dedD<>kan* P_{204}::*gfp-damX*) showing that GFP-DamX localization is independent of DedD and that *gfp-damX* rescues division when induced with 0.01 mM IPTG but causes striking filamentation in cells with this background grown with 0.1 mM IPTG. Bar, 5 μm.

served before and after eviction of the *kan* cassette were identical (data not shown).

These findings distinguish DamX, DedD, and RlpA from the only previously studied *E. coli* SPOR domain protein, FtsN, which is essential, although its SPOR domain is not (13, 26, 65). Could the importance of the new SPOR domain proteins be masked because they compensate for one another? To pursue this possibility, we constructed a redundant set of dou-

TABLE 3. Localization of GFP-DamX in strains with *fts* mutant backgrounds

Strain background[a]	Temp (°C)	NaCl[b]	Sugar[c]	No. of cells evaluated	Avg length (μm) (SD)	Total no. of rings	% of cells with ring(s)	Ring spacing[d]
WT	30	+	−	164	4.1 (1.1)	136	82	5
	42	−	−	178	4.5 (1.6)	233	92	3
ftsZ(Ts)	30	+	−	258	7.7 (2.2)	220	76	9
	42	−	−	194	34.2 (18.5)	7	4	947
ftsA(Ts)	30	+	−	168	7.1 (2)	217	96	6
	42	−	−	160	33.5 (7.3)	446	98	12
ftsQ(Ts)	30	+	−	128	13.9 (5.9)	339	99	5
	42	−	−	126	28.9 (14.2)	350	90	10
ftsI(Ts)	30	+	−	134	7.8 (2.8)	145	94	7
	42	−	−	117	29.8 (9.3)	368	97	10
FtsN^{DEP}	30	+	Ara	208	5.4 (1.5)	187	83	6
	30	+	Glu	155	36.6 (15.2)	744	99	8

[a] Strains used were EC2138, EC2140, EC2142, EC2144, EC2146, and EC2148. WT, wild type; FtsN^{DEP}, FtsN depletion.
[b] Either 1 or 0% NaCl.
[c] Either 0.2% L-arabinose (Ara) or 0.2% D-glucose (Glu).
[d] Total length of cells (or filaments) divided by total number of GFP-DamX rings. This normalization procedure facilitates comparison of wild-type and mutant strains.

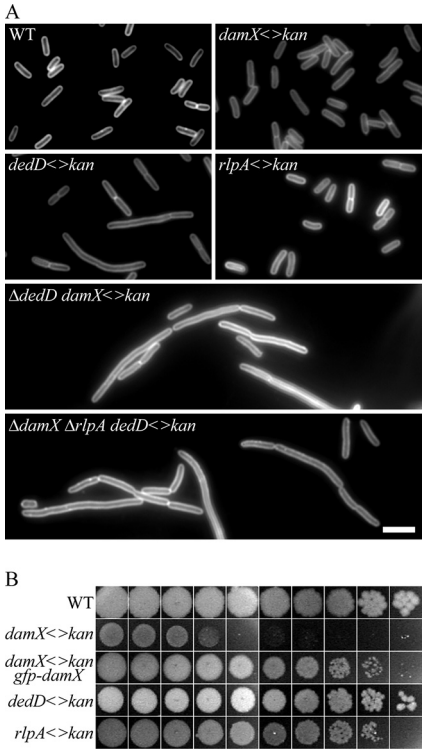

FIG. 5. Phenotypes of *damX*, *dedD*, and *rlpA* mutants. (A) Micrographs of FM4-64-stained cells with the indicated genotypes. The white bar represents 5 μm. Cells were grown in LB medium at 30°C for at least six mass doublings and fixed. The strains shown are BW25113 (WT), JW3351 (*damX<>kan*), JW3578 (*dedD<>kan*), JW0628 (*rlpA<>kan*), EC1926 (Δ*dedD damX<>kan*), and EC2152 (Δ*damX* Δ*rlpA dedD<>kan*). (B) Sensitivity to deoxycholate. Stationary-phase cultures were adjusted to an OD_{600} of 1.0, and then fourfold serial dilutions were spotted onto LB0N agar plates containing 0.1% deoxycholate and 10 μM IPTG. Strains shown are BW25113, JW3351, EC2130, JW3578, and JW0628.

ble and triple mutants. (By redundant, we mean that *damX<>kan* was introduced by transduction into a Δ*dedD* mutant and *dedD<>kan* was introduced into a Δ*damX* mutant, etc.) The *damX dedD* double mutants had striking division defects, with an average length of ~16 μm and over 15% of the cells exhibiting multiple constrictions (Fig. 5A; Table 4). Adding an *rlpA* mutation to the mix had no discernible effect on cell length or propensity for chaining (Fig. 5A; Table 4). This pattern is unlikely to be an artifact of the mutants' having acquired suppressor mutations because we also constructed Δ*damX* Δ*rlpA dedD<>kan*/pBAD33-*damX* depletion strains, which upon extensive depletion, behaved like the simple triple mutants (data not shown).

In the course of these studies, we noticed that the division defects in the mutants were growth phase dependent. The mutants continued to divide in stationary phase, so they were about the same length as wild-type cells after being grown overnight. The cell lengths reported in Table 4 were recorded after cells were grown for six doublings in LB medium at 30°C. Maintaining the cultures in exponential growth by repeated dilution into fresh medium did not result in further elongation (data not shown).

DamX interacts with multiple Fts proteins in a bacterial two-hybrid system. Using a bacterial two-hybrid system based on reconstitution of an adenylate cyclase (38, 39), we observed that DamX interacts strongly with itself, FtsQ, and FtsN (Fig. 6). Weaker interactions with FtsZ, FtsA, FtsI, and possibly FtsL were detected (Fig. 6). It should be noted that the interactions of DamX with itself and FtsZ could be tested only in one configuration; in the case of FtsZ, this is because the gene is tolerated only in the low-copy-number pKT25 plasmid.

DamX antagonizes FtsQ. Because cells with a *damX* null mutation had no obvious division defect, we introduced the mutation into various *fts* mutant backgrounds by transduction in the expectation that some combinations might prove synthetically lethal or cause cell sickness. The mutations combined with *damX<>kan* were the *ftsZ84*(Ts), *ftsA12*(Ts), *zipA1*(Ts),

TABLE 4. Division phenotypes of mutants lacking *damX*, *dedD*, and/or *rlpA*[a]

Strain	Genotype	No. of cells evaluated	Avg length (μm) (SD)	% of cells >10 μm long	% of cells with no. of constrictions:		
					0	1	>1
BW25113	Wild type	241	3.7 (1.0)	0	77	23	0
JW3351	*damX<>kan*	306	3.9 (1.0)	0	78	22	1
JW3578	*dedD<>kan*	301	6.1 (7.9)	7	58	35	7
JW0628	*rlpA<>kan*	297	3.9 (1.1)	0	81	18	1
EC1916	Δ*damX rlpA<>kan*	310	3.8 (0.9)	0			
EC1920	Δ*rlpA damX<>kan*	335	4.0 (1.1)	0			
EC1918	Δ*dedD rlpA<>kan*	235	6.3 (4.7)	10			
EC1922	Δ*rlpA dedD<>kan*	296	7.0 (4.5)	8			
EC1924	Δ*damX dedD<>kan*	268	18 (15)	61	45	37	18
EC1926	Δ*dedD damX<>kan*	286	15 (14)	46	50	34	16
EC2150	Δ*damX* Δ*rlpA dedD<>kan*	379	15 (13)	45			
EC2152	Δ*damX* Δ*rlpA dedD<>kan*	284	19 (18)	53	47	35	18
EC2154	Δ*damX* Δ*dedD rlpA<>kan*	273	19 (15)	62	45	32	23
EC2177	Δ*damX dedD<>kan* P_{204}::*gfp-damX*	277	5.0 (1.8)	4			
EC251	Wild type	539	3.4 (1.0)	0			
EC1910	*damX<>kan*	528	3.8 (1.0)	0			
EC1912	*dedD<>kan*	467	6.7 (5.1)	7			
EC1914	*rlpA<>kan*	525	3.9 (1.1)	0			

[a] Cells were grown for six doublings to an OD_{600} of ~0.5, fixed, stained with FM4-64, and photographed using fluorescence microscopy.

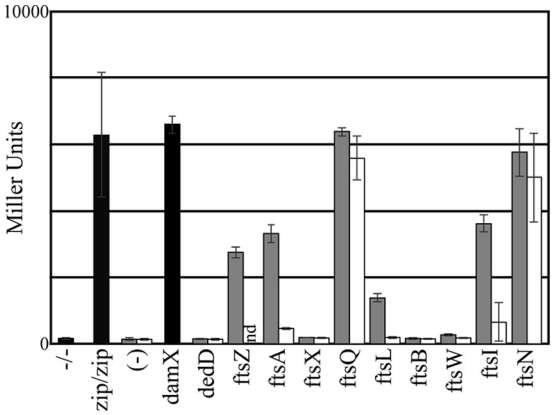

FIG. 6. Findings from the bacterial two-hybrid assay of DamX interactions with itself and other division proteins. Transformants of DHM1 harboring derivatives of pUT18c and pKT25 were grown in LB medium containing ampicillin and kanamycin plus 0.5 mM IPTG to an OD_{600} of 0.6 to 0.8 and assayed for β-galactosidase activity. Bars represent the means and standard deviations of results from at least three independent experiments. Black bars indicate results for the empty vector control harboring pUT18c and pKT25 (−/−), the positive control harboring pKT25-*zip* and pUT18-*zip* (zip/zip), and the homodimerization sample with pKT25-*damX* and pUT18c-*damX* (damX). Results for other samples are shown as pairs of gray and white bars reflecting the two potential genetic configurations, pKT25-*damX*/pUT18c-*fts* (gray) and pKT25-*fts*/pUT18c-*damX* (white). (−), empty vector control; nd, not determined (because the high-copy-number *ftsZ* plasmid is not stably maintained).

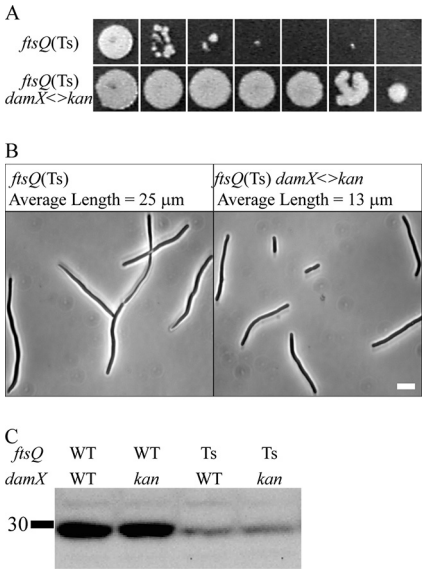

FIG. 7. Loss of *damX* ameliorates the *ftsQ1*(Ts) phenotype. (A) Plating efficiency. Tenfold serial dilutions of cells with the indicated genotypes were spotted onto LB0N agar and incubated at 42°C. (B) Cell division. Cells of EC303 or EC1992 were fixed and photographed 1 h after being shifted to LB0N medium at 42°C. Average lengths are based on measurements of 120 cells from each strain. Bar, 5 μm. (C) Western blot showing levels of FtsQ 1 h after shifting of EC251, EC1910, EC303, and EC1992 cells to LB0N medium at 42°C. The 30-kDa mass marker is indicated to the left of the blot.

ftsQ1(Ts), and *ftsI23*(Ts) mutations. The double mutants were assayed for viability by spotting serial dilutions onto plates containing LB or LB0N medium, and the plates were incubated overnight at 30, 37, and 42°C. To our surprise, the only synthetic phenotype we observed was rescue of an *ftsQ1*(Ts) mutant. We got the same result with four independent *damX<>kan ftsQ1*(Ts) isolates, which argues that the loss of *damX* rather than an unrecognized suppressor mutation is responsible for amelioration of the temperature-sensitive phenotype. The *damX<>kan* allele improved the plating efficiency of an *ftsQ1*(Ts) strain by about 10^6-fold on LB0N medium at 42°C (Fig. 7A). Moreover, when liquid cultures where shifted from 30 to 42°C, the *ftsQ1*(Ts) single mutant exhibited more extensive filamentation than the *damX<>kan ftsQ1*(Ts) double mutant (Fig. 7B). The two strains grew at the same rate after the shift to 42°C, indicating that the double mutant was shorter because it divided more efficiently, not because it grew more slowly. Western blotting revealed that the presence or absence of DamX had no effect on the level of FtsQ1(Ts) protein (Fig. 7C), which was present in very small amounts, as reported previously (6). Efforts to introduce an *ftsQ*::Tn*phoA50* (Kan^r) null mutation (7) into a *damX* strain were unsuccessful, suggesting that the loss of DamX facilitates division by resulting in small amounts of FtsQ rather than by bypassing the requirement for FtsQ altogether (data not shown). This possibility was confirmed by constructing a Δ*damX ftsQ*::Tn*phoA50* (Kan^r)/pBAD33-*ftsQ* depletion strain. The depletion strain required arabinose for viability, and the terminal phenotype when the strain was grown in the presence of glucose to prevent *ftsQ* expression was extensive filamentation (data not shown).

DISCUSSION

DamX, DedD, and RlpA are new septal ring proteins. This study has identified three new *E. coli* septal ring proteins: DamX, DedD, and RlpA (Fig. 2). We have also shown that *damX* and *dedD* mutants have division defects, either alone or in combination with mutations in other division genes, demonstrating that DamX and DedD are division proteins (Fig. 5 and 7; Table 4). In the case of RlpA, however, we have so far failed to uncover a phenotype that proves the protein is actually involved in cytokinesis. Follow-up experiments revealed that numerous SPOR domains localize to division sites and bind PG (Fig. 3). Remarkably, even a SPOR domain from *Aquifex* localizes to division sites when produced in the heterologous host *E. coli*. This finding argues that septal localization of SPOR domains extends even to the deepest branch in the bacterial tree and that whatever targets SPOR domains to the septal ring is conserved in species from *E. coli* to *Aquifex*. Finally, we have characterized the DamX protein in some detail, showing that it interacts with several division proteins in a bacterial two-hybrid system and appears to antagonize FtsQ (Fig. 4, 6, and 7; Table 3).

Implications of SPOR domain localization to septal rings. The finding that SPOR domains themselves localize to division sites has several interesting implications. First, we infer that many of the >1,500 SPOR domain proteins in the Pfam database are likely to be involved in cell division. Indeed, it was recently shown that SPOR domain proteins localize to division sites in *C. crescentus*, *Burkholderia thailandensis*, and *Myxococcus xanthus* (49). Moreover, we have observed that VPA1294-RFP localizes to division sites when produced in *V. parahae-*

molyticus swimmer cells (R. Kustusch and D. Weiss, unpublished data). Nevertheless, we doubt that all proteins that contain SPOR domains are involved in cell division because, for example, CwlC of *B. subtilis* has been implicated in sporulation (41, 61). Second, as discussed in more detail below, the SPOR domains studied here probably localize by binding to septal PG, which in turn implies that septal PG is different from lateral wall PG. Following up on this observation may lead to novel insights into PG metabolism during cytokinesis. Third, the SPOR domains are quite divergent at the level of amino acid sequence. An alignment of the seven SPOR domains investigated here revealed that only the amino acids at one position, which corresponds to residue Q251 in FtsN, are identical in all proteins (Fig. 1B). Yet these seven SPOR domains all localize to the midcell. It will be interesting to learn how proteins with such different sequences bind to the same PG structure. Alternatively, should it turn out that different SPOR domains bind to different sites, there must be a multitude of differences between septal and lateral wall PGs.

Several of the preceding remarks are predicated on the inference that SPOR domains localize by binding to septal PG, and we realize that this inference remains to be proven. The current paradigm is that septal ring assembly is driven by a complex web of protein-protein interactions (29, 38, 66). We do not think SPOR domains are likely to conform to this paradigm because it is difficult to imagine what septal ring protein in *E. coli* could be conserved highly enough to be recognized by SPOR domains from *B. subtilis* (26), *C. hutchinsonii*, and *A. aeolicus*. Genes for widely conserved potential interaction partners such as FtsQ and FtsI are difficult or impossible to identify in the *Cytophaga* and *Aquifex* genomes (45; S. J. Arends and D. Weiss, unpublished data). Moreover, the analysis of the SPOR domain from DamX under way in our laboratory indicates that mutations that impair septal localization also impair binding to PG sacculi in the pulldown assay (K. Williams and D. Weiss, unpublished data). For these reasons, we suspect that SPOR domains target a form of PG that is transiently present at the division site, as also suggested by Gerding et al. (26).

This possibility raises the question of how septal PG differs from PG in the lateral wall or at the cell poles. Published analyses have come to different conclusions, but the general consensus appears to be that any differences are minor (17, 36, 53, 56, 60). Nevertheless, there is a clear consensus that the division site is a zone of intense PG synthesis during constriction (19, 69). It is therefore likely that some forms of PG, such as glycan strands that have been extended but not yet cross-linked, pentapeptide side chains, PG with a paucity of covalently attached Lpp, intermediates in PG turnover, and multilayered PG, may be more abundant in septal regions.

Gerding et al. suggested that SPOR domains target a specific PG turnover intermediate, namely, glycan strands that lack peptide side chains (26). Naked glycan strands would arise if amidases ran ahead of lytic transglycosylases during PG degradation. Gerding et al. based this suggestion on their finding that SPOR domains did not localize to septal regions in an *E. coli* strain devoid of amidases (26) and on a report from Vollmer's group that the purified SPOR domain from FtsN binds to naked glycan strands generated by amidase treatment of isolated sacculi (65). In that study, FtsN′s SPOR domain did not bind to muropeptides or to free peptides (65), although it should be noted that glycan strands that carried peptides were not tested. It is also worth noting that a subsequent paper from Vollmer's group reported binding of FtsN′s SPOR domain to muropeptides (50). The basis for this contradiction was not discussed but may have to do with the fact that in the second study the muropeptides contained 1,6-anhydromuramic acid ends owing to the use of a different enzyme to degrade the sacculi. Finally, to our knowledge, disaccharides indicative of naked glycan strands have never turned up in analyses of the muropeptide composition of PG, implying either that they do not exist or that the analytical methods are not adequate to detect them. Clearly, more work will be needed to test the hypothesis that SPOR domains bind preferentially to glycan strands that lack peptide side chains.

DamX. The first report on *damX* noted that overexpression inhibits cell division (43). This characteristic appears to distinguish DamX from other bitopic membrane proteins involved in cell division in *E. coli*. Why is DamX (apparently) different? One possibility is that DamX's SPOR domain impairs processing of septal PG when the domain is present in excess, as indicated by the fact that GFP-SPOR domain fusion proteins impair division to some extent (Fig. 3). But this hypothesis does not readily explain why excess FtsN is well tolerated. A second possibility is that excess DamX excludes much of the FtsN from the septal ring. A third potential explanation is that DamX sequesters FtsQ. Consistent with this hypothesis, we found that DamX interacted strongly with FtsQ in a bacterial two-hybrid system (Fig. 6), the expression of a *gfp-damX* fusion in cells with an *ftsQ1*(Ts) background impaired division even at the permissive temperature (Fig. 4), and a *damX* null mutation rescued an *ftsQ1*(Ts) mutant at the nonpermissive temperature (Fig. 7). The same *damX* null mutation did not rescue any of the other temperature-sensitive mutants tested—the *ftsZ84*, *ftsA12*, *zipA1*, and *ftsI23* mutants (data not shown). The *damX* mutation had no obvious effect on the stability of the FtsQ1(Ts) protein. Taken together, these findings suggest that DamX antagonizes FtsQ function. Nevertheless, the fact that the loss of *damX* exacerbates the division defect of *dedD* mutants implies that DamX also contributes positively to cytokinesis (Fig. 5).

Complementary approaches point to DamX being an early recruit in the hypothetical pathway for assembly of the septal ring. Roughly 80% of the cells in a population growing in LB with a doubling time of ~35 min exhibited septal localization of DamX-GFP (Fig. 2A; Table 3). These frequencies are similar to what has been reported for FtsZ, FtsA, and ZipA. For comparison, late recruits such as FtsQ, FtsI, and FtsN typically localize to the midcell in only 40 to 50% of the population. We also observed that recruitment of DamX-GFP to the septal ring required FtsZ but not FtsA or proteins downstream of FtsA (Fig. 4; Table 3). These findings, together with our observation of weak interactions of DamX with FtsZ and FtsA in the two-hybrid system (Fig. 6), raise the intriguing possibility that DamX links the Z ring directly to the PG layer. In this context, it is worth noting that the cytoplasmic domain of DamX is predicted to be both large (Fig. 1A) and highly charged—103 aa, with 34 Asp or Glu and 24 Arg or Lys.

One context in which the SPOR domain of DamX may cause misinterpretation of experimental results is the two-hy-

brid system. We observed that DamX interacts with itself and FtsN (Fig. 6). This pattern may reflect colocalization to a PG site rather than direct protein-protein interaction, although if this is the case, it is interesting that DamX did not interact with DedD. The DedD fusions used in the two-hybrid study are at least partially functional in the sense that they interact with some Fts proteins (Williams and Weiss, unpublished).

DedD. Of the three new septal ring proteins described here, DedD is arguably the most important in that a simple *dedD* null mutant had discernible division defects whereas mutants lacking either *damX* or *rlpA* were normal in length (Fig. 4). DedD had interesting genetic interactions with DamX. The deletion of *damX* in a *dedD* background accentuated the division defect, as did the expression of a *gfp-damX* fusion. One potential explanation is that DedD protects FtsQ from DamX by competing with DamX for localization to the septal ring, perhaps because DedD and DamX target the same sites on PG. Nevertheless, DedD did not interact with DamX in the two-hybrid system (Fig. 6), even though such an interaction would be expected if DedD and DamX are attracted to the same PG sites.

RlpA. RlpA is perhaps the most enigmatic of the *E. coli* SPOR domain proteins because null mutants have no obvious phenotype and even combining an *rlpA* mutation with mutations in *damX* and *dedD* had no discernible effect. Nevertheless, we doubt that RlpA is an innocent bystander at the septal ring. The most obvious role for RlpA would be to link the outer membrane to the PG during constriction. As this role is also fulfilled by Pal (27) and perhaps by other proteins such as OmpA and Lpp, it is possible that synthetic phenotypes will emerge if *rlpA* mutations are combined with mutations affecting these other outer membrane proteins.

Gerding et al. observed localization of RlpA both to the septal ring and to foci at various cites along the cell cylinder (26), whereas we observed RlpA only in septal rings. We think it is important to note that our charge-coupled device camera is inferior to theirs for imaging of RFP. A role for *rlpA* in elongation would make sense because it resides on the chromosome next to other genes that encode proteins involved in morphogenesis, namely, *pbpA*, *rodA*, and *dacA* (62).

ACKNOWLEDGMENTS

We thank William Margolin, Craig Ellermeier, and Lucy Shapiro for antibodies, Greg Phillips for an mCherry plasmid, D. RayChaudhuri for pET-3Z$^+$, Adam Okerlund for assistance purifying FtsZ, Gouzel Karimova and Daniel Ladant for bacterial two-hybrid plasmids and strains, and an anonymous reviewer for insightful comments that improved the manuscript. We gratefully acknowledge the National BioResource Project (NIG, Japan) for Keio collection mutants. We are grateful to Linda McCarter for calling our attention to VPA1294 and DamX, and to Piet de Boer and Janine Maddock, who shared results prior to publication.

This work was supported by a grant (no. GM083975) to D.S.W. from the National Institutes of Health. R.J.S. and S.R. were supported by NSF REU in Microbiology at The University of Iowa (through grant no. 064798). The DNA facility is supported through the Holden Comprehensive Cancer Center's cancer center support grant 2 P30 CA086862 from the National Cancer Institute/NIH and the Carver College of Medicine, The University of Iowa.

REFERENCES

1. **Arends, S. J., R. J. Kustusch, and D. S. Weiss.** 2009. ATP-binding site lesions in FtsE impair cell division. J. Bacteriol. **191:**3772–3784.
2. **Baba, T., T. Ara, M. Hasegawa, Y. Takai, Y. Okumura, M. Baba, K. A. Datsenko, M. Tomita, B. L. Wanner, and H. Mori.** 2006. Construction of *Escherichia coli* K-12 in-frame, single-gene knockout mutants: the Keio collection. Mol. Syst. Biol. **2:**2006 0008.
3. **Bass, S., Q. Gu, and A. Christen.** 1996. Multicopy suppressors of *prc* mutant *Escherichia coli* include two HtrA (DegP) protease homologs (HhoAB), DksA, and a truncated R1pA. J. Bacteriol. **178:**1154–1161.
4. **Bernhardt, T. G., and P. A. de Boer.** 2003. The *Escherichia coli* amidase AmiC is a periplasmic septal ring component exported via the twin-arginine transport pathway. Mol. Microbiol. **48:**1171–1182.
5. **Boussau, B., L. Gueguen, and M. Gouy.** 2008. Accounting for horizontal gene transfers explains conflicting hypotheses regarding the position of aquificales in the phylogeny of Bacteria. BMC Evol. Biol. **8:**272.
6. **Buddelmeijer, N., M. E. Aarsman, A. H. Kolk, M. Vicente, and N. Nanninga.** 1998. Localization of cell division protein FtsQ by immunofluorescence microscopy in dividing and nondividing cells of *Escherichia coli*. J. Bacteriol. **180:**6107–6116.
7. **Carson, M. J., J. Barondess, and J. Beckwith.** 1991. The FtsQ protein of *Escherichia coli*: membrane topology, abundance, and cell division phenotypes due to overproduction and insertion mutations. J. Bacteriol. **173:**2187–2195.
8. **Chen, J. C., and J. Beckwith.** 2001. FtsQ, FtsL and FtsI require FtsK, but not FtsN, for co-localization with FtsZ during *Escherichia coli* cell division. Mol. Microbiol. **42:**395–413.
9. **Chen, J. C., P. H. Viollier, and L. Shapiro.** 2005. A membrane metalloprotease participates in the sequential degradation of a *Caulobacter* polarity determinant. Mol. Microbiol. **55:**1085–1103.
10. **Chen, J. C., D. S. Weiss, J. M. Ghigo, and J. Beckwith.** 1999. Septal localization of FtsQ, an essential cell division protein in *Escherichia coli*. J. Bacteriol. **181:**521–530.
11. **Cherepanov, P. P., and W. Wackernagel.** 1995. Gene disruption in *Escherichia coli*: TcR and KmR cassettes with the option of Flp-catalyzed excision of the antibiotic-resistance determinant. Gene **158:**9–14.
12. **Cormack, B. P., R. H. Valdivia, and S. Falkow.** 1996. FACS-optimized mutants of the green fluorescent protein (GFP). Gene **173:**33–38.
13. **Dai, K., Y. Xu, and J. Lutkenhaus.** 1993. Cloning and characterization of *ftsN*, an essential cell division gene in *Escherichia coli* isolated as a multicopy suppressor of *ftsA12*(Ts). J. Bacteriol. **175:**3790–3797.
14. **Dai, K., Y. Xu, and J. Lutkenhaus.** 1996. Topological characterization of the essential *Escherichia coli* cell division protein FtsN. J. Bacteriol. **178:**1328–1334.
15. **Datsenko, K. A., and B. L. Wanner.** 2000. One-step inactivation of chromosomal genes in *Escherichia coli* K-12 using PCR products. Proc. Natl. Acad. Sci. U. S. A. **97:**6640–6645.
16. **Deckert, G., P. V. Warren, T. Gaasterland, W. G. Young, A. L. Lenox, D. E. Graham, R. Overbeek, M. A. Snead, M. Keller, M. Aujay, R. Huber, R. A. Feldman, J. M. Short, G. J. Olsen, and R. V. Swanson.** 1998. The complete genome of the hyperthermophilic bacterium *Aquifex aeolicus*. Nature **392:**353–358.
17. **de Jonge, B. L., F. B. Wientjes, I. Jurida, F. Driehuis, J. T. Wouters, and N. Nanninga.** 1989. Peptidoglycan synthesis during the cell cycle of *Escherichia coli*: composition and mode of insertion. J. Bacteriol. **171:**5783–5794.
18. **den Blaauwen, T., M. A. de Pedro, M. Nguyen-Distèche, and J. A. Ayala.** 2008. Morphogenesis of rod-shaped sacculi. FEMS Microbiol. Rev. **32:**321–344.
19. **de Pedro, M. A., J. C. Quintela, J. V. Höltje, and H. Schwarz.** 1997. Murein segregation in *Escherichia coli*. J. Bacteriol. **179:**2823–2834.
20. **Draper, G. C., N. McLennan, K. Begg, M. Masters, and W. D. Donachie.** 1998. Only the N-terminal domain of FtsK functions in cell division. J. Bacteriol. **180:**4621–4627.
21. **Eberhardt, C., L. Kuerschner, and D. S. Weiss.** 2003. Probing the catalytic activity of a cell division-specific transpeptidase in vivo with beta-lactams. J. Bacteriol. **185:**3726–3734.
22. **Errington, J., R. A. Daniel, and D. J. Scheffers.** 2003. Cytokinesis in bacteria. Microbiol. Mol. Biol. Rev. **67:**52–65, table of contents.
23. **Finn, R. D., J. Tate, J. Mistry, P. C. Coggill, S. J. Sammut, H. R. Hotz, G. Ceric, K. Forslund, S. R. Eddy, E. L. Sonnhammer, and A. Bateman.** 2008. The Pfam protein families database. Nucleic Acids Res. **36:**D281–D288.
24. **Geissler, B., and W. Margolin.** 2005. Evidence for functional overlap among multiple bacterial cell division proteins: compensating for the loss of FtsK. Mol. Microbiol. **58:**596–612.
25. **Gerdes, S. Y., M. D. Scholle, J. W. Campbell, G. Balazsi, E. Ravasz, M. D. Daugherty, A. L. Somera, N. C. Kyrpides, I. Anderson, M. S. Gelfand, A. Bhattacharya, V. Kapatral, M. D'Souza, M. V. Baev, Y. Grechkin, F. Mseeh, M. Y. Fonstein, R. Overbeek, A. L. Barabasi, Z. N. Oltvai, and A. L. Osterman.** 2003. Experimental determination and system level analysis of essential genes in *Escherichia coli* MG1655. J. Bacteriol. **185:**5673–5684.
26. **Gerding, M. A., B. Liu, F. O. Bendezu, C. A. Hale, T. G. Bernhardt, and P. A. de Boer.** 2009. Self-enhanced accumulation of FtsN at division sites and roles for other proteins with a SPOR domain (DamX, DedD, and RlpA) in *Escherichia coli* cell constriction. J. Bacteriol. **191:**7303–7401.
27. **Gerding, M. A., Y. Ogata, N. D. Pecora, H. Niki, and P. A. de Boer.** 2007. The

trans-envelope Tol-Pal complex is part of the cell division machinery and required for proper outer-membrane invagination during cell constriction in *E. coli*. Mol. Microbiol. **63:**1008–1025.
28. **Glauner, B.** 1988. Separation and quantification of muropeptides with high-performance liquid chromatography. Anal. Biochem. **172:**451–464.
29. **Goehring, N. W., and J. Beckwith.** 2005. Diverse paths to midcell: assembly of the bacterial cell division machinery. Curr. Biol. **15:**R514–R526.
30. **Goehring, N. W., C. Robichon, and J. Beckwith.** 2007. Role for the nonessential N terminus of FtsN in divisome assembly. J. Bacteriol. **189:**646–649.
31. **González-Castro, M. J., J. López-Hernández, J. Simal-Lozano, and M. J. Oruña-Concha.** 1997. Determination of amino acids in green beans by derivitization with phenylisothiocyanate and high-performance liquid chromatography with ultraviolet detection. J. Chromatogr. Sci. **35:**181–185.
32. **Guzman, L. M., D. Belin, M. J. Carson, and J. Beckwith.** 1995. Tight regulation, modulation, and high-level expression by vectors containing the arabinose pBAD promoter. J. Bacteriol. **177:**4121–4130.
33. **Guzman, L. M., D. S. Weiss, and J. Beckwith.** 1997. Domain-swapping analysis of FtsI, FtsL, and FtsQ, bitopic membrane proteins essential for cell division in *Escherichia coli*. J. Bacteriol. **179:**5094–5103.
34. **Haldimann, A., and B. L. Wanner.** 2001. Conditional-replication, integration, excision, and retrieval plasmid-host systems for gene structure-function studies of bacteria. J. Bacteriol. **183:**6384–6393.
35. **Heidrich, C., A. Ursinus, J. Berger, H. Schwarz, and J. V. Höltje.** 2002. Effects of multiple deletions of murein hydrolases on viability, septum cleavage, and sensitivity to large toxic molecules in *Escherichia coli*. J. Bacteriol. **184:**6093–6099.
36. **Ishidate, K., A. Ursinus, J. V. Höltje, and L. Rothfield.** 1998. Analysis of the length distribution of murein glycan strands in *ftsZ* and *ftsI* mutants of *E. coli*. FEMS Microbiol. Lett. **168:**71–75.
37. **Jonczyk, P., R. Hines, and D. W. Smith.** 1989. The *Escherichia coli dam* gene is expressed as a distal gene of a new operon. Mol. Gen. Genet. **217:**85–96.
38. **Karimova, G., N. Dautin, and D. Ladant.** 2005. Interaction network among *Escherichia coli* membrane proteins involved in cell division as revealed by bacterial two-hybrid analysis. J. Bacteriol. **187:**2233–2243.
39. **Karimova, G., J. Pidoux, A. Ullmann, and D. Ladant.** 1998. A bacterial two-hybrid system based on a reconstituted signal transduction pathway. Proc. Natl. Acad. Sci. U. S. A. **95:**5752–5756.
40. **Karimova, G., A. Ullmann, and D. Ladant.** 2001. Protein-protein interaction between *Bacillus stearothermophilus* tyrosyl-tRNA synthetase subdomains revealed by a bacterial two-hybrid system. J. Mol. Microbiol. Biotechnol. **3:**73–82.
41. **Kuroda, A., Y. Asami, and J. Sekiguchi.** 1993. Molecular cloning of a sporulation-specific cell wall hydrolase gene of *Bacillus subtilis*. J. Bacteriol. **175:**6260–6268.
42. **Lewenza, S., D. Vidal-Ingigliardi, and A. P. Pugsley.** 2006. Direct visualization of red fluorescent lipoproteins indicates conservation of the membrane sorting rules in the family *Enterobacteriaceae*. J. Bacteriol. **188:**3516–3524.
43. **Lyngstadaas, A., A. Lobner-Olesen, and E. Boye.** 1995. Characterization of three genes in the *dam*-containing operon of *Escherichia coli*. Mol. Gen. Genet. **247:**546–554.
44. **Makino, K., K. Oshima, K. Kurokawa, K. Yokoyama, T. Uda, K. Tagomori, Y. Iijima, M. Najima, M. Nakano, A. Yamashita, Y. Kubota, S. Kimura, T. Yasunaga, T. Honda, H. Shinagawa, M. Hattori, and T. Iida.** 2003. Genome sequence of *Vibrio parahaemolyticus*: a pathogenic mechanism distinct from that of *V. cholerae*. Lancet **361:**743–749.
45. **Margolin, W.** 2000. Themes and variations in prokaryotic cell division. FEMS Microbiol. Rev. **24:**531–548.
46. **Mercer, K. L., and D. S. Weiss.** 2002. The *Escherichia coli* cell division protein FtsW is required to recruit its cognate transpeptidase, FtsI (PBP3), to the division site. J. Bacteriol. **184:**904–912.
47. **Miller, J. H.** 1972. Experiments in molecular genetics. Cold Spring Harbor Laboratory, Cold Spring Harbor, NY.
48. **Mishima, M., T. Shida, K. Yabuki, K. Kato, J. Sekiguchi, and C. Kojima.** 2005. Solution structure of the peptidoglycan binding domain of *Bacillus subtilis* cell wall lytic enzyme CwlC: characterization of the sporulation-related repeats by NMR. Biochemistry **44:**10153–10163.
49. **Möll, A., and M. Thanbichler.** 2009. FtsN-like proteins are conserved components of the cell division machinery in proteobacteria. Mol. Microbiol. **72:**1037–1053.
50. **Müller, P., C. Ewers, U. Bertsche, M. Anstett, T. Kallis, E. Breukink, C. Fraipont, M. Terrak, M. Nguyen-Distèche, and W. Vollmer.** 2007. The essential cell division protein FtsN interacts with the murein (peptidoglycan) synthase PBP1B in *Escherichia coli*. J. Biol. Chem. **282:**36394–36402.
51. **Nagasawa, H., Y. Sakagami, A. Suzuki, H. Suzuki, H. Hara, and Y. Hirota.** 1989. Determination of the cleavage site involved in C-terminal processing of penicillin-binding protein 3 of *Escherichia coli*. J. Bacteriol. **171:**5890–5893.
52. **Nonet, M. L., C. C. Marvel, and D. R. Tolan.** 1987. The *hisT-purF* region of the *Escherichia coli* K-12 chromosome. Identification of additional genes of the *hisT* and *purF* operons. J. Biol. Chem. **262:**12209–12217.
53. **Obermann, W., and J. V. Höltje.** 1994. Alterations of murein structure and of penicillin-binding proteins in minicells from *Escherichia coli*. Microbiology **140**(Pt. 1)**:**79–87.
54. **Pichoff, S., and J. Lutkenhaus.** 2002. Unique and overlapping roles for ZipA and FtsA in septal ring assembly in *Escherichia coli*. EMBO J. **21:**685–693.
55. **RayChaudhuri, D., and J. T. Park.** 1992. *Escherichia coli* cell-division gene *ftsZ* encodes a novel GTP-binding protein. Nature **359:**251–254.
56. **Romeis, T., U. Kohlrausch, K. Burgdorf, and J. V. Höltje.** 1991. Murein chemistry of cell division in *Escherichia coli*. Res. Microbiol. **142:**325–332.
57. **Rudd, K. E.** 2000. EcoGene: a genome sequence database for *Escherichia coli* K-12. Nucleic Acids Res. **28:**60–64.
58. **Samaluru, H., L. SaiSree, and M. Reddy.** 2007. Role of SufI (FtsP) in cell division of *Escherichia coli*: evidence for its involvement in stabilizing the assembly of the divisome. J. Bacteriol. **189:**8044–8052.
59. **Shaner, N. C., R. E. Campbell, P. A. Steinbach, B. N. Giepmans, A. E. Palmer, and R. Y. Tsien.** 2004. Improved monomeric red, orange and yellow fluorescent proteins derived from *Discosoma* sp. red fluorescent protein. Nat. Biotechnol. **22:**1567–1572.
60. **Signoretto, C., F. Di Stefano, and P. Canepari.** 1996. Modified peptidoglycan chemical composition in shape-altered *Escherichia coli*. Microbiology **142**(Pt. 8)**:**1919–1926.
61. **Smith, T. J., and S. J. Foster.** 1995. Characterization of the involvement of two compensatory autolysins in mother cell lysis during sporulation of *Bacillus subtilis* 168. J. Bacteriol. **177:**3855–3862.
62. **Takase, I., F. Ishino, M. Wachi, H. Kamata, M. Doi, S. Asoh, H. Matsuzawa, T. Ohta, and M. Matsuhashi.** 1987. Genes encoding two lipoproteins in the *leuS-dacA* region of the *Escherichia coli* chromosome. J. Bacteriol. **169:**5692–5699.
63. **Tarry, M., S. J. Arends, P. Roversi, E. Piette, F. Sargent, B. C. Berks, D. S. Weiss, and S. M. Lea.** 2009. The *Escherichia coli* cell division protein and model Tat substrate SufI (FtsP) localizes to the septal ring and has a multicopper oxidase-like structure. J. Mol. Biol. **386:**504–519.
64. **Tenorio, E., T. Saeki, K. Fujita, M. Kitakawa, T. Baba, H. Mori, and K. Isono.** 2003. Systematic characterization of *Escherichia coli* genes/ORFs affecting biofilm formation. FEMS Microbiol. Lett. **225:**107–114.
65. **Ursinus, A., F. van den Ent, S. Brechtel, M. de Pedro, J. V. Höltje, J. Löwe, and W. Vollmer.** 2004. Murein (peptidoglycan) binding property of the essential cell division protein FtsN from *Escherichia coli*. J. Bacteriol. **186:**6728–6737.
66. **Vicente, M., A. I. Rico, R. Martinez-Arteaga, and J. Mingorance.** 2006. Septum enlightenment: assembly of bacterial division proteins. J. Bacteriol. **188:**19–27.
67. **Weiss, D. S.** 2004. Bacterial cell division and the septal ring. Mol. Microbiol. **54:**588–597.
68. **Weiss, D. S., J. C. Chen, J. M. Ghigo, D. Boyd, and J. Beckwith.** 1999. Localization of FtsI (PBP3) to the septal ring requires its membrane anchor, the Z ring, FtsA, FtsQ, and FtsL. J. Bacteriol. **181:**508–520.
69. **Wientjes, F. B., and N. Nanninga.** 1989. Rate and topography of peptidoglycan synthesis during cell division in *Escherichia coli*: concept of a leading edge. J. Bacteriol. **171:**3412–3419.
70. **Wissel, M. C., and D. S. Weiss.** 2004. Genetic analysis of the cell division protein FtsI (PBP3): amino acid substitutions that impair septal localization of FtsI and recruitment of FtsN. J. Bacteriol. **186:**490–502.
71. **Xie, G., D. C. Bruce, J. F. Challacombe, O. Chertkov, J. C. Detter, P. Gilna, C. S. Han, S. Lucas, M. Misra, G. L. Myers, P. Richardson, R. Tapia, N. Thayer, L. S. Thompson, T. S. Brettin, B. Henrissat, D. B. Wilson, and M. J. McBride.** 2007. Genome sequence of the cellulolytic gliding bacterium *Cytophaga hutchinsonii*. Appl. Environ. Microbiol. **73:**3536–3546.
72. **Yang, J. C., F. Van Den Ent, D. Neuhaus, J. Brevier, and J. Löwe.** 2004. Solution structure and domain architecture of the divisome protein FtsN. Mol. Microbiol. **52:**651–660.